DCG

GJBX-99(78)

MONITORING OF THE AIRPORT CALIBRATION PADS AT WALKER FIELD, GRAND JUNCTION, COLORADO FOR LONG-TERM RADIATION VARIATIONS

Bendix Field Engineering Corporation
Grand Junction Operations
Grand Junction, Colorado 81501

August 1978

PREPARED FOR THE U.S. DEPARTMENT OF ENERGY
GRAND JUNCTION OFFICE
UNDER CONTRACT NO. EY-76-C-13-1664

GJBX-99(78)

MONITORING OF THE AIRPORT CALIBRATION PADS AT WALKER FIELD, GRAND JUNCTION, COLORADO FOR LONG-TERM RADIATION VARIATIONS

David C. Stromswold

BENDIX FIELD ENGINEERING CORPORATION
Grand Junction Operations
Grand Junction, Colorado 81501

August 1978

PREPARED FOR THE U.S. DEPARTMENT OF ENERGY
GRAND JUNCTION OFFICE
UNDER CONTRACT NO. EY-76-C-13-1664

CONTENTS

ILLUSTRATIONS

TABLES

MONITORING OF THE AIRPORT CALIBRATION PADS AT WALKER FIELD, GRAND JUNCTION, COLORADO FOR LONG-TERM RADIATION VARIATIONS

SUMMARY

Monitoring of radiation from the U.S. Department of Energy Calibration Pads located at Walker Field Airport, Grand Junction, Colorado has been initiated to detect possible long-term variations in the radioactive character of the pads. A NaI detector is being used to collect spectral data over the energy range 0.5 MeV to 3 MeV. For the first 7 months of the monitoring, the period covered by this report, an increase of approximately 10 percent in the apparent uranium concentration of the pads was detected during the winter of 1978. This increase is attributed to radon buildup in the pads due to meteorological effects. Information is also presented on the physical description of the pads, their radiometric concentrations and uniformity, and the effects of rainwater on observed radiation.

INTRODUCTION

This report describes the initial monitoring of the airborne systems calibration pads located at Walker Field Airport, Grand Junction, Colorado, U.S.A. The method of monitoring and the results are presented for the period October 1977 to April 1978.

The radiation from the pads was monitored to detect possible long-term changes in the radioactive character of the pads. Some of the causes that might lead to these changes are radon variations in the pads due to meteorological effects, moisture differences due to wet and dry periods, and chemical changes within the pads. Such variations in the radiation have in fact been reported for pads located in Denmark (Løvborg et al, 1978). The report was based on total-count gamma-ray measurements taken on the pads at Risø; variations were seen only on the pad with high uranium content (198 ppm eU).

DESCRIPTION OF AIRPORT PADS

Physical

Large pads suitable for use in calibrating airborne gamma-ray spectrometers were constructed in November 1976. Selected radioactive ores were mixed with concrete to obtain large-area sources that emit the following energy gamma rays of interest in uranium exploration: 1.76 MeV from ^{214}Bi (a decay product of uranium), 2.61 MeV from ^{208}Tl (a decay product of thorium), and 1.46 MeV from ^{40}K. Each pad has surface dimensions 30 feet x 40 feet (9.1 meters x 12.2 meters) and a thickness of 1.5 feet (0.5 meters). There are a total of five pads with various concentrations of potassium, uranium, and thorium. Pad 1 is a background pad with elemental concentrations limited to those naturally occurring in the concrete used to make the pads. Pads 2, 3, and 4 contain enhanced concentrations of potassium, thorium, and uranium, respectively. Pad 5 contains a mixture of all three elements in relatively high concentrations. The physical layout of the pads is shown in Figure 1. Construction details for the pads are described in another report (Ward, 1978).

Concentrations

Samples of the pad material were collected during construction. Seventy samples were obtained from selected locations in each pad. The radiometric energy spectra of these samples were measured using a NaI spectrometer and compared to those of known-concentration samples from the New Brunswick Laboratory, U.S. Department of Energy. Concentrations of potassium, uranium, and thorium in the 70 samples were determined from the comparison data. The concentrations of the samples from each pad were weighted to give greater importance to samples taken from the surface of the pads. Gamma rays originating from the bottom of the pads are attenuated as they pass upward; hence, the gamma rays originating near the surface of the pads contribute more to the total measured radioactivity than do the gamma rays from the bottom of the pads. By using an exponential weighting factor for the samples taken from different depths within the pads, the effects of gamma-ray attenuation by the concrete for the various gamma-ray energies are included in the assigned concentrations of potassium, uranium, and thorium. These concentrations are given in Table 1. The statistical uncertainties given in the table are the 95 percent confidence intervals (two standard deviations) obtained from the weighted sample concentrations. These uncertainties arise from concentration variations among the samples from each pad. The statistical uncertainties for the individual samples are not included in the table because they are much smaller than the uncertainties due to variations among the 70 samples.

Uniformity

In dealing with large-area radiation sources such as the airport pads, concern exists regarding the uniformity of the radiation over the surface area. For this reason, a survey was conducted on each pad with a

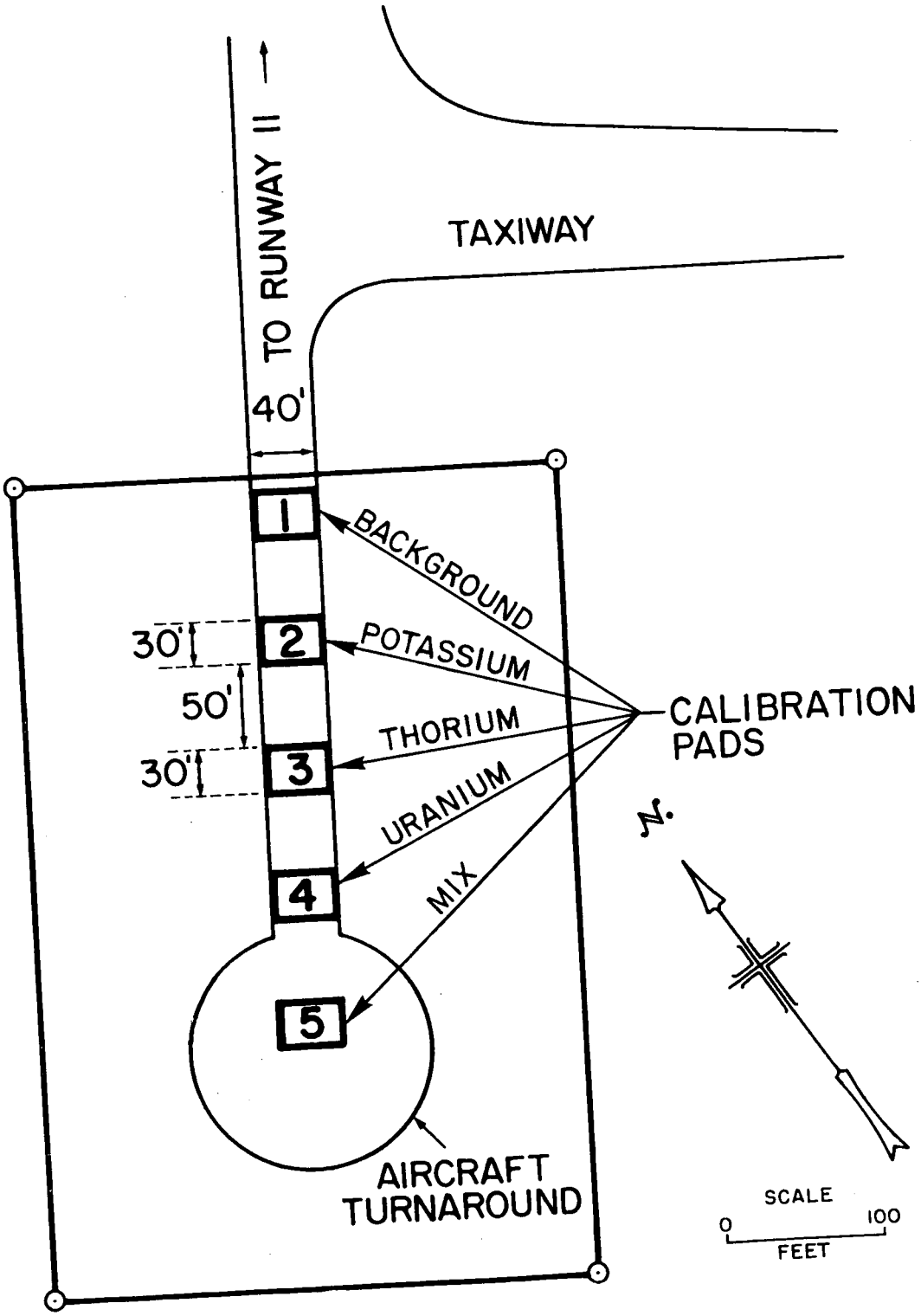

FIGURE 1.
DOE CALIBRATION PADS, WALKER FIELD AIRPORT
GRAND JUNCTION, COLORADO

TABLE 1.
AIRPORT PAD CONCENTRATIONS AND DENSITIES
WALKER FIELD AIRPORT, GRAND JUNCTION, COLORADO

PAD	CONCENTRATION			
	%K	ppm U	ppm Th	Density
1	1.45 ± 0.01	2.2 ± 0.1	6.3 ± 0.1	1.91 ± 0.00
2	5.14 ± 0.09	5.1 ± 0.3	8.5 ± 0.3	2.00 ± 0.01
3	2.01 ± 0.04	5.1 ± 0.2	45.3 ± 0.7	1.92 ± 0.00
4	2.03 ± 0.05	30.3 ± 1.6	9.2 ± 0.3	1.91 ± 0.00
5	4.11 ± 0.06	20.4 ± 1.3	17.5 ± 0.3	1.97 ± 0.00

Note: Statistical uncertainties quoted are the 95 percent confidence intervals.

NaI detector to determine the uniformity in the potassium, uranium, and thorium data. Measurements were made at 5 foot (1.52 meter) intervals along a rectangular grid. The data obtained from these measurements show some minor variations in the radiation over the surface, but there are no significant differences. An example of the uniformity data is shown in Figure 2, where uranium counts on Pad 4 are plotted. At the edges of the pad, the detector is sensitive to radiation from both the pad and the adjoining ground, and the decrease in counts recorded at the edges is due to the lower natural radioactivity of the ground.

Effects of Standing Water

The pads are not covered, and rainwater can collect on them. The effects of water standing on the pads have been determined by comparing data taken before and after rain. These data are shown in Table 2. The observed decrease in potassium and thorium counts for the wet pads closely approximates the amount of gamma-ray attenuation predictable from the 3/16 inch (0.5 cm) of water standing on the pads. It thus appears that the effect of moisture soaking into the pads is minimal and that removal of standing water would return the counts to normal. The rise in uranium counts for the wet pads is attributed to radon-gas entrapment below the water, which, in this case, had been standing on the pads for approximately 20 hours. Radon is a decay product of uranium in the chain that leads to ^{214}Bi whose 1.76 MeV gamma ray is used to indicate the presence of uranium. ^{214}Bi can also build up at ground level from the decay of ^{214}Pb which has been swept out of the atmosphere by the rain. ^{214}Pb decays with a half-life of 27 minutes into ^{214}Bi; thus, the ^{214}Pb is reduced to negligible levels within 2.5 hours (five half-lives) after a rain. Because the data for the wet pads were collected several hours after the rain stopped, and the half-life of ^{214}Bi is only 20 minutes, removal of ^{214}Pb from the atmosphere by rain is probably not the origin of the enhanced uranium counts.

MONITORING

Data Collection

During the first few months of monitoring, measurements were taken twice per month. The frequency of measurement was subsequently reduced because it was observed that monthly measurements were adequate for detecting radiation variations caused by seasonal climate changes and aging of the pads.

The detector used for the monitoring is a NaI crystal, 11.5 inches (29.2 cm) in diameter and 4 inches (10.2 cm) thick, coupled to seven photomultiplier tubes. It is mounted in a well-insulated container to reduce the possibility of rapid temperature changes damaging the detector or causing equipment instabilities. Tests of the system's insulation have shown that the rate of temperature change inside the container is only 2°C per hour for a temperature difference of 20°C between the container's exterior and interior. (The crystal manufacturer specifies 10°C per hour as the maximum rate of temperature change to which the detector can be subjected without damage.) The location of the detector within the insulating container places it approximately 7 inches (18 cm) above the ground surface.

During data collection, the detector is placed at the center of the pads and all other equipment is located in a support truck parked off the pads to minimize disturbances to the measurements. Coaxial cable is used to transmit the gamma-ray pulses from the preamplifier on the detector to the truck for signal processing. A block diagram of the electronic system is shown in Figure 3, and a picture of the monitoring system in operation is shown in Figure 4.

A multichannel analyzer (MCA) is used to record the spectral data in 1024 channels; the energy region investigated is approximately 500 keV to 3000 keV. The 1461 keV peak from ^{40}K (potassium peak), the 1764 keV peak from ^{214}Bi ("uranium" peak), and the 2614 keV peak from ^{208}Tl ("thorium" peak) appear distinctly in the spectra of all pads. A typical segment of a spectrum which includes these peaks is shown in Figure 5.

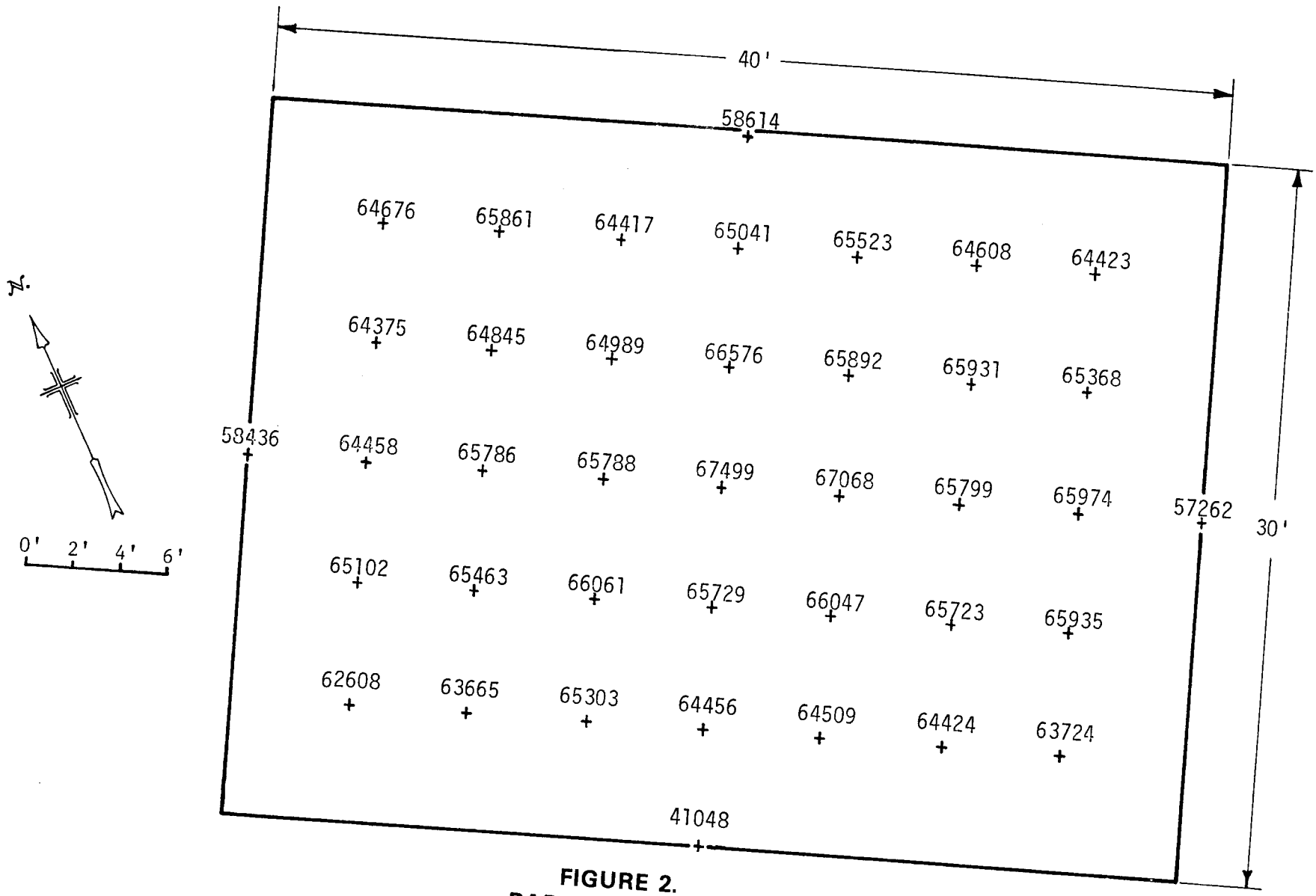

FIGURE 2.
PAD UNIFORMITY

Counts were obtained on Pad 4 in the uranium energy window.
(Counting time = 400 seconds.)

TABLE 2.
COMPARISON DATA FOR PADS WET AND DRY

(Counts obtained in 600 seconds using a 1024 cubic inch NaI detector)

Peak		Pad #1	Pad #2	Pad #3	Pad #4	Pad #5
K	Dry	152,528	409,838	283,682	383,329	475,348
	Wet	150,530	393,292	278,963	367,031	463,912
U	Dry	43,374	66,286	124,221	233,122	190,202
	Wet	44,200	68,657	126,294	229,241	190,831
T	Dry	28,299	35,679	150,565	47,922	72,546
	Wet	28,164	36,025	150,023	46,990	72,123

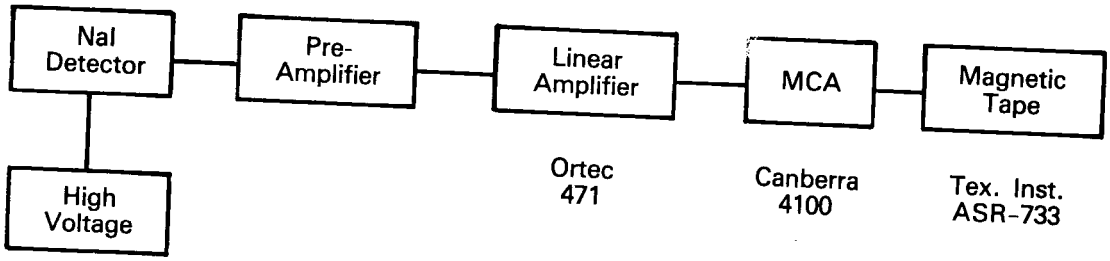

FIGURE 3.
BLOCK DIAGRAM OF ELECTRONIC SYSTEM

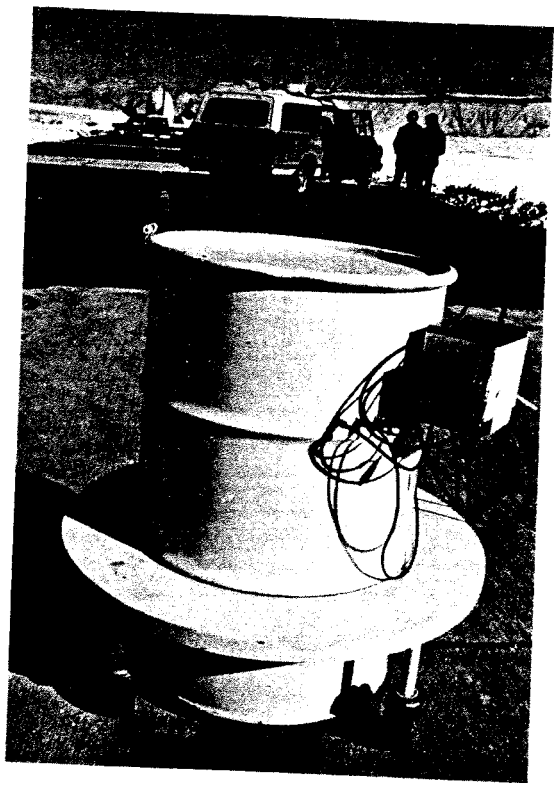

FIGURE 4.
MONITORING SYSTEM

The radiation detector is located in the barrel, and the supporting electronics are in the truck. The airplane in the background is calibrating its radiation detection system.

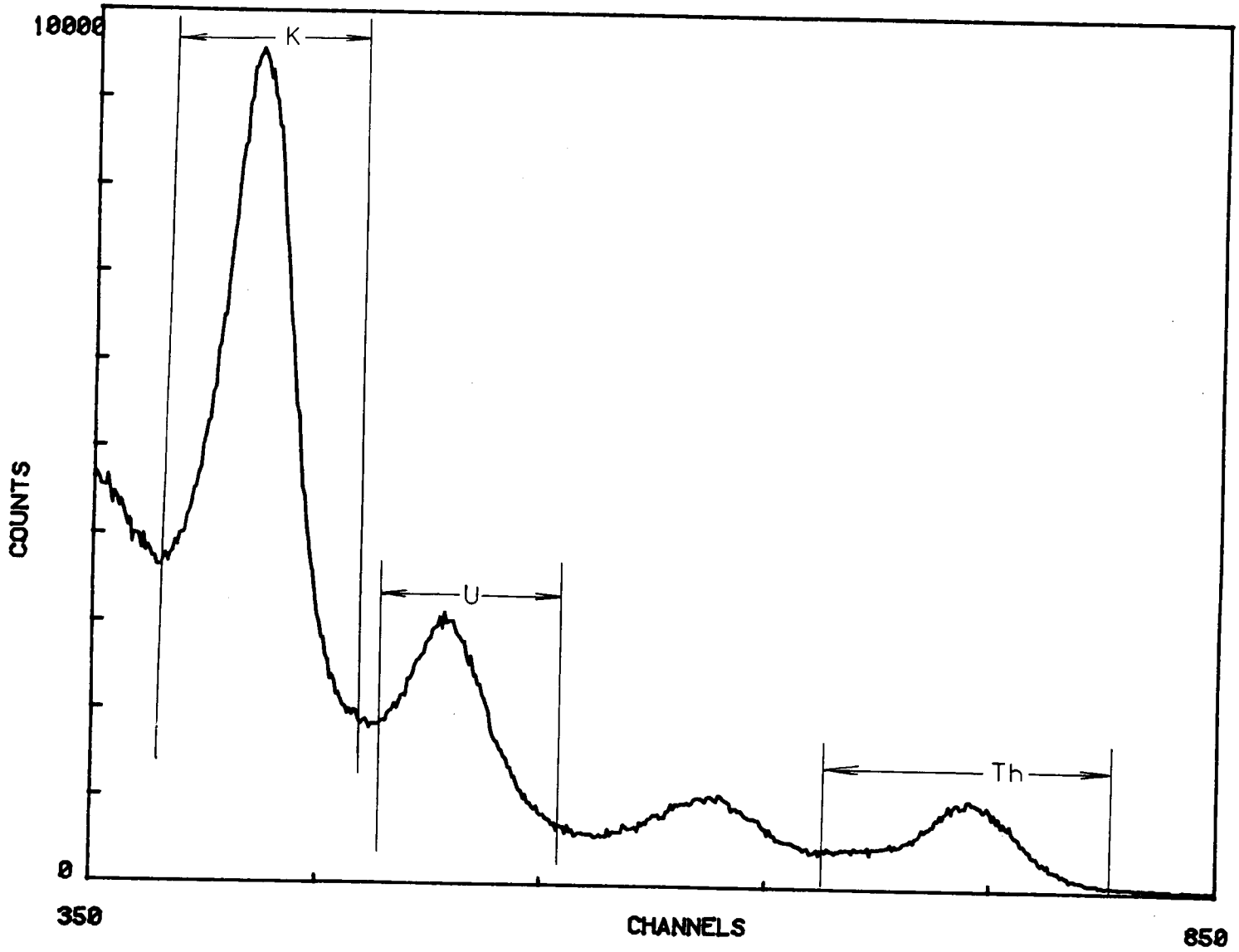

FIGURE 5.
TYPICAL NaI SPECTRUM FROM PADS SHOWING K, U, AND Th PEAKS
Counts are plotted versus channel number of multichannel analyzer.

The length of data collection is 1000 seconds for pads 2, 3, 4, and 5, but for pad 1 (the background pad) it is 1600 seconds. This longer collection time compensates for the lower count rate from pad 1 and gives approximately the same statistical precision in the data from all pads. During analysis, the different counting times are removed by dividing by time to get counts per second.

The spectra are transferred to magnetic tape in the truck using a Texas Instruments ASR-733 cassette recording system. Header information, including pad number, counting time, and date, is added to the tape using the keyboard of the ASR-733.

Results

The tapes recorded at the airport are transcribed to magnetic cartridges on a Tektronics 4051 graphics computer, and these cartridges are then used to enter the data into the computer for analysis. Several programs have been written to assist in this analysis. One progrm provides an energy calibration that converts channel number to energy using a linear least-squares fit:

$$E = a + bx,$$

where

E = energy (keV)

x = channel number

a and b = fitting constants.

Values of the fitting constants are determined using the potassium, uranium, and thorium peaks in the spectrum.

Plots of the spectra over various energy ranges are available from the computer program, and examples of these plots are given in Figures 6 through 10 for the five pads. The different concentrations of potassium, uranium, and thorium in the individual pads are clearly reflected in the different peak heights in the figures.

A second program sums the counts in the peaks to give integrated K, U, Th, and total counts (T.C.). This summing is carried out over fixed energy ranges rather than over channels in order to remove long-term drifts in the electronic equipment. The energy ranges for the summations are:

K = 1300 keV to 1640 keV
U = 1640 keV to 2000 keV
Th = 2425 keV to 2850 keV
T.C. = 1300 keV to 2850 keV.

The summed data for the various collection dates have been divided by time to obtain count rates; these count rates are given in Table 3. The statistical uncertainties shown in the table are two standard deviations (95 percent confidence intervals) from the radiation counting. In some cases the fluctuations in the count rates exceed the statistical limits but do not appear to follow a trend. These fluctuations are due, at least in part, to the difficulty of obtaining good energy calibration from the broad peaks produced by the NaI detector. A trend is evident on pad 4 for the count rate in the uranium peak: count rates are elevated during the months of December through March. In particular, the count rate rises from 219.60 counts/second in October 1977 to 240.38 counts/second in January 1978, and then it decreases to 213.11 counts/second in April 1978. Similar variations in the uranium peak can be seen for pads 2, 3, and 5, although they are less pronounced for these pads, which contain lower concentrations of uranium.

Discussion

The data in Table 3 are not stripped; that is, the counts in each peak include the full-energy gamma ray from the main source of interest plus Compton-scattered gamma rays from other sources. For this reason, it is difficult to attribute observed changes in the count rates to changes in individual, elemental concentrations. However, it is possible to calculate stripping factors and sensitivities for a detector's response to potassium, uranium, and thorium using data recorded from sources of known concentrations. These response characteristics were calculated (Stromswold and Kosanke, 1978) using the data in

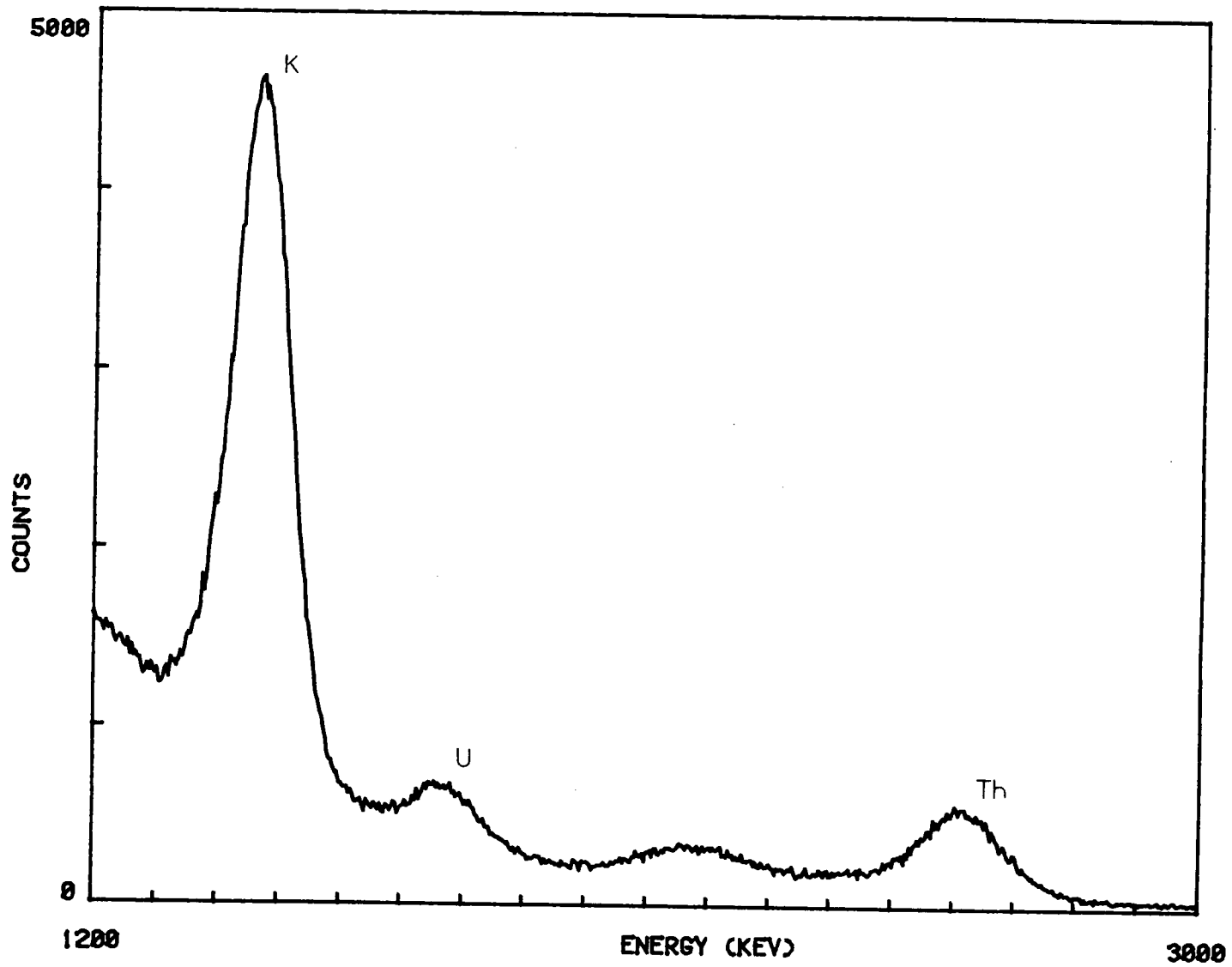

FIGURE 6.
SPECTRUM OF PAD 1 SHOWING K, U, AND Th PEAKS

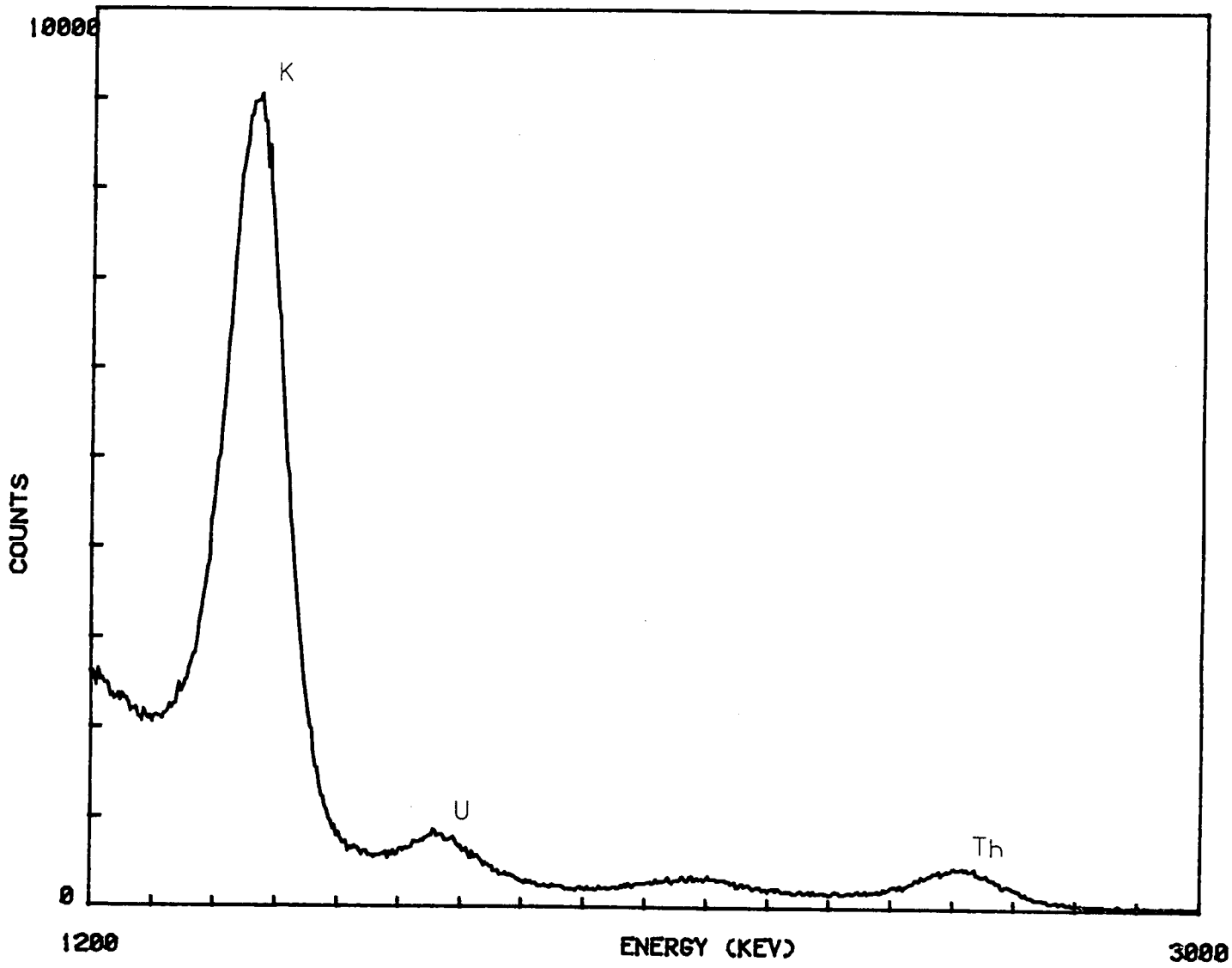

FIGURE 7.
SPECTRUM OF PAD 2 SHOWING K, U, AND Th PEAKS

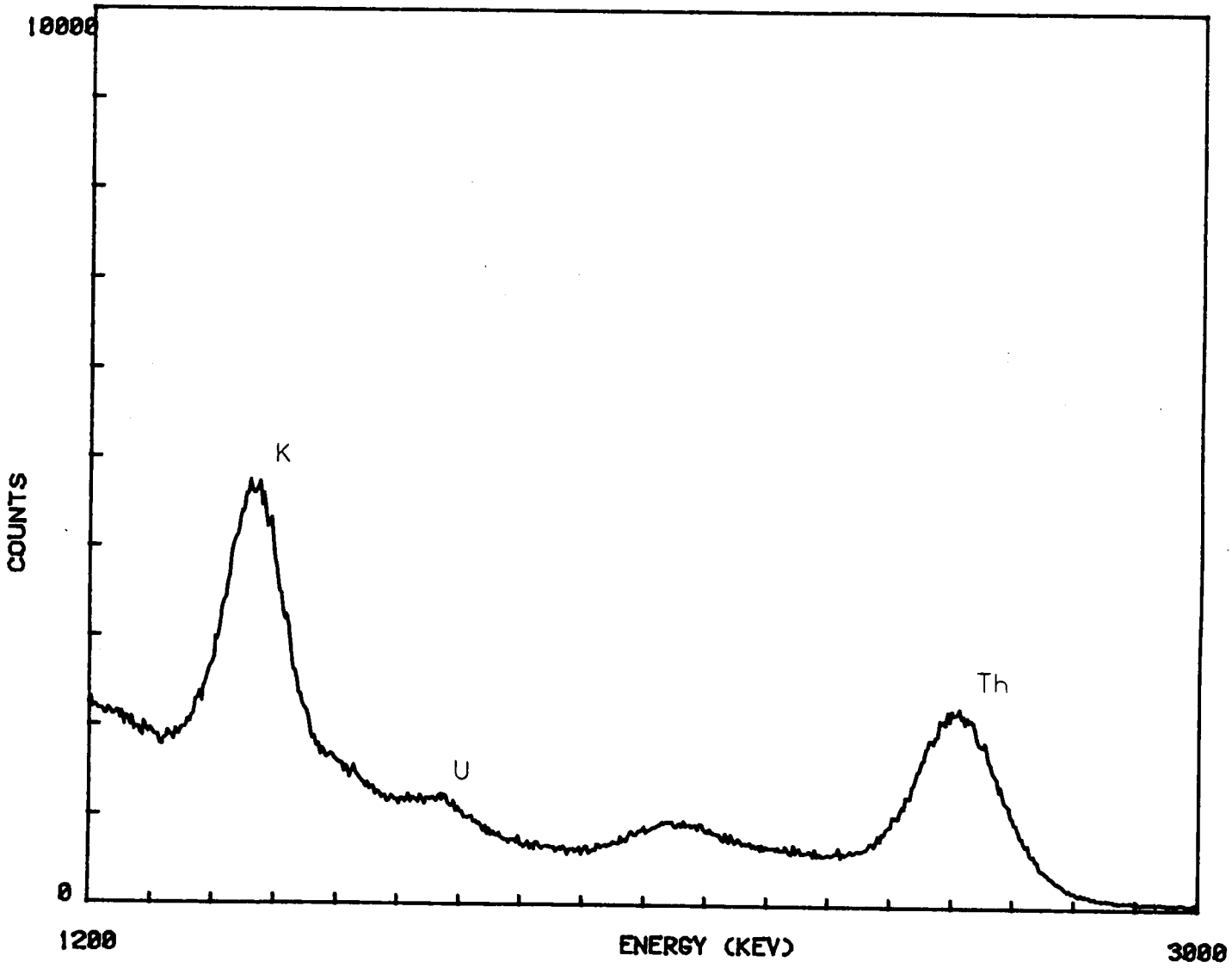

FIGURE 8.
SPECTRUM OF PAD 3 SHOWING K, U, AND Th PEAKS

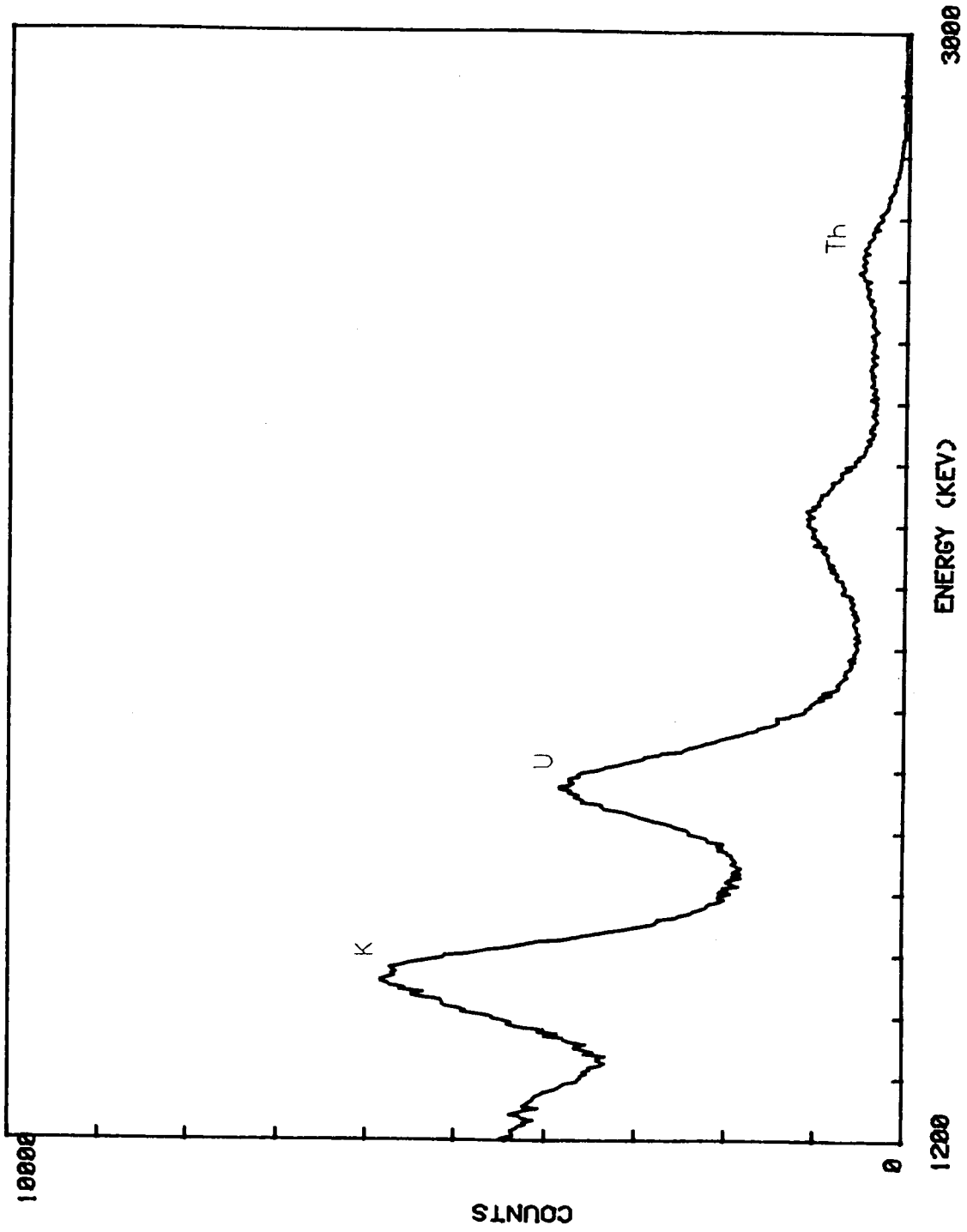

FIGURE 9.
SPECTRUM OF PAD 4 SHOWING K, U, AND Th PEAKS

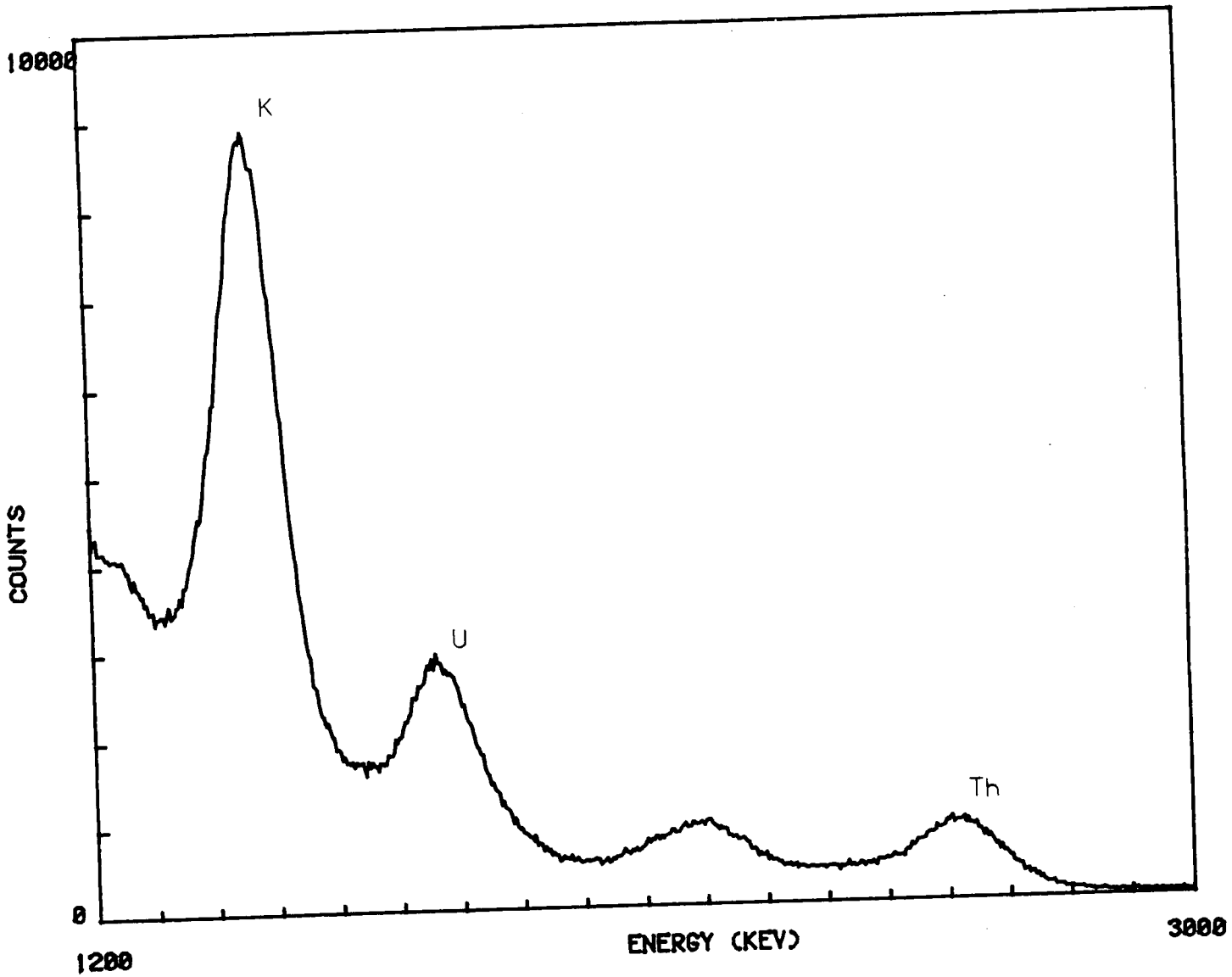

FIGURE 10.
SPECTRUM OF PAD 5 SHOWING K, U, AND Th PEAKS

TABLE 3.
COUNT RATES OBTAINED ON THE PADS
(counts/seconds)

PAD	PEAK	Date					
		10/17,77	10/31/77	11/18/77	12/01/77	12/14/77	01/09/78
1	K	150.48 ± 0.61	147.22 ± 0.61	*	146.47 ± 0.61	148.61 ± 0.61	147.49 ± 0.61
	U	34.63 ± 0.29	34.11 ± 0.29	*	32.12 ± 0.28	33.58 ± 0.29	34.94 ± 0.30
	Th	23.11 ± 0.24	23.19 ± 0.24	*	23.33 ± 0.24	22.41 ± 0.24	22.53 ± 0.24
	T.C.	228.25 ± 0.76	224.75 ± 0.75	*	222.32 ± 0.75	224.59 ± 0.75	225.13 ± 0.75
2	K	426.83 ± 1.31	422.35 ± 1.30	428.63 ± 1.31	420.43 ± 1.30	422.28 ± 1.30	421.58 ± 1.30
	U	57.22 ± 0.48	59.23 ± 0.49	58.14 ± 0.48	56.54 ± 0.48	57.12 ± 0.48	59.83 ± 0.49
	Th	29.83 ± 0.35	29.94 ± 0.35	32.38 ± 0.36	29.81 ± 0.35	29.70 ± 0.34	29.08 ± 0.34
	T.C.	543.30 ± 1.47	541.42 ± 1.47	550.29 ± 1.48	536.98 ± 1.47	538.63 ± 1.47	539.92 ± 1.47
3	K	293.96 ± 1.08	284.98 ± 1.07	291.22 ± 1.08	287.08 ± 1.07	292.75 ± 1.08	286.61 ± 1.07
	U	111.65 ± 0.67	109.82 ± 0.66	110.09 ± 0.67	108.61 ± 0.66	112.41 ± 0.67	111.38 ± 0.67
	Th	139.03 ± 0.75	139.03 ± 0.75	139.97 ± 0.75	136.40 ± 0.74	136.18 ± 0.74	136.57 ± 0.74
	T.C.	635.77 ± 1.59	625.96 ± 1.58	633.72 ± 1.59	625.00 ± 1.58	632.72 ± 1.59	625.10 ± 1.58
4	K	398.95 ± 1.26	388.13 ± 1.25	407.72 ± 1.28	406.57 ± 1.28	407.85 ± 1.28	408.65 ± 1.28
	U	219.60 ± 0.94	222.17 ± 0.94	224.40 ± 0.95	230.32 ± 1.96	229.99 ± 1.96	235.04 ± 1.97
	Th	39.44 ± 0.40	40.06 ± 0.40	41.83 ± 0.41	40.54 ± 0.40	39.98 ± 0.40	39.75 ± 0.40
	T.C.	736.02 ± 1.72	729.40 ± 1.71	754.90 ± 1.74	760.03 ± 1.74	757.94 ± 1.74	765.41 ± 1.75
5	K	495.94 ± 1.41	494.86 ± 1.41	500.24 ± 1.41	496.64 ± 1.41	503.14 ± 1.42	500.46 ± 1.41
	U	171.80 ± 0.83	178.97 ± 0.85	175.88 ± 0.84	179.80 ± 0.85	180.34 ± 0.85	182.45 ± 0.85
	Th	63.14 ± 0.50	63.22 ± 0.50	62.84 ± 0.50	62.48 ± 0.50	63.04 ± 0.50	61.85 ± 0.50
	T.C.	806.38 ± 1.80	815.42 ± 1.81	818.07 ± 1.81	817.52 ± 1.81	824.71 ± 1.82	822.33 ± 1.81

PAD	PEAK	Date				
		01/25/78	02/03/78	03/08/78	04/07/78	04/12/78
1	K	149.34 ± 0.61	149.17 ± 0.61	143.78 ± 0.60	141.54 ± 0.59	141.54 ± 0.59
	U	36.33 ± 0.30	34.66 ± 0.29	30.92 ± 0.28	28.66 ± 0.27	28.37 ± 0.27
	Th	22.50 ± 0.24	22.62 ± 0.24	22.29 ± 0.24	22.41 ± 0.24	22.15 ± 0.24
	T.C.	228.86 ± 0.76	226.66 ± 0.75	216.26 ± 0.74	211.24 ± 0.73	210.95 ± 0.73
2	K	423.88 ± 1.36	420.59 ± 1.30	417.34 ± 1.29	416.73 ± 1.29	414.47 ± 1.29
	U	61.46 ± 0.50	57.36 ± 0.48	55.19 ± 0.47	50.78 ± 0.45	50.11 ± 0.45
	Th	28.72 ± 0.34	28.70 ± 0.34	28.88 ± 0.34	29.09 ± 0.34	29.10 ± 0.34
	T.C.	544.03 ± 1.48	535.13 ± 1.46	530.33 ± 1.46	524.65 ± 1.45	521.08 ± 1.44
3	K	288.64 ± 1.07	285.22 ± 1.07	283.27 ± 1.06	282.88 ± 1.06	279.16 ± 1.06
	U	115.53 ± 0.68	110.24 ± 0.66	106.63 ± 0.65	105.20 ± 0.65	101.87 ± 0.64
	Th	136.06 ± 0.74	135.85 ± 0.74	134.94 ± 0.73	135.19 ± 0.74	135.23 ± 0.74
	T.C.	631.44 ± 1.59	621.08 ± 1.58	615.37 ± 1.57	613.24 ± 1.57	606.13 ± 1.56
4	K	419.44 ± 1.30	403.88 ± 1.27	410.25 ± 1.28	394.34 ± 1.26	387.23 ± 1.24
	U	240.38 ± 1.96	232.10 ± 1.96	232.08 ± 1.96	216.80 ± 0.93	213.11 ± 0.92
	Th	39.28 ± 0.40	38.68 ± 0.39	39.01 ± 0.39	37.91 ± 0.39	38.31 ± 0.39
	T.C.	783.51 ± 1.77	756.72 ± 1.74	763.53 ± 1.75	727.68 ± 1.71	715.67 ± 1.69
5	K	500.20 ± 1.41	501.38 ± 1.42	497.43 ± 1.41	482.68 ± 1.39	482.92 ± 1.39
	U	187.69 ± 0.87	183.22 ± 0.86	179.50 ± 0.85	166.71 ± 0.82	164.94 ± 0.81
	Th	61.92 ± 0.50	61.50 ± 0.50	61.60 ± 0.50	61.41 ± 0.50	61.89 ± 0.50
	T.C.	829.02 ± 1.82	824.46 ± 1.82	816.25 ± 1.81	785.01 ± 1.77	783.31 ± 1.77

NOTE: Statistical uncertainties quoted are the 95% confidence intervals.
* Data unavailable due to magnetic tape error

Table 3 to determine an average response for the monitoring period. Based on this detector response, the count-rate data for the individual dates were used to calculate the concentrations of potassium, uranium, and thorium shown in Table 4. The statistical uncertainties given in Table 4 are those related to the original counting data; uncertainties in the detector's response function are not included because they are constant for all the dates and tend to obscure the actual variations. (The concentrations in Table 4 are slightly higher than those given in Table 1 because background counts have not been removed.) The data in Table 4 are plotted in Figures 11 through 15 for the five pads. For potassium and thorium there is little or no trend in the concentrations for the monitoring period. However, on pads 4 and 5 there is a significant increase in apparent uranium concentration for the winter months, the highest values being obtained in January. The variations are well above the statistical uncertainties, and they represent approximately 10 percent changes in the apparent uranium concentration.

These changes are attributed to variation of the radon (Rn) concentrations within the pads. The inert gas ^{222}Rn is a decay product of ^{238}U and is free to migrate from the site of decay during its 3.8 day half-life. The radon which escapes from the pads decreases the apparent uranium concentration of the pads because the 1.76 MeV gamma ray used as a measure of uranium actually comes from ^{214}Bi, a decay product of radon. The data in Table 4 suggest that the radon in the pads was not constant; rather, it increased during the winter months to produce the enhanced apparent uranium concentration.

The possibility exists that the enhanced uranium readings were due to background changes not directly related to the pads. However, by subtracting background count rates, the influences external to the pads and detector system can be removed. The results of such a subtraction, using the data taken on pad 1 as background, are given in Table 5. The increase in apparent uranium concentration is still evident even though the statistical uncertainties have increased as a result of the subtraction. The apparent uranium concentrations of pad 4 after background subtraction are plotted in Figure 16. The amount of the change is still seen to be approximately 10 percent; thus, background variations did not artificially produce the enhanced count rates.

Finally, the possibility of time-dependent changes in the gamma-ray detection system must be considered. Such changes, for whatever reason they might occur, can produce artificial variations in the calculated concentrations of the pads. These changes would affect all three concentrations (potassium, uranium, and thorium) and not just the uranium concentration. The fact that systematic variations were seen only for uranium suggests that the detection system is not the origin of these variations. The thorium concentrations provide a means for assuring the detector's stability because there is no reason the thorium concentration should change in time. (The only gas in the decay chain of thorium is ^{220}Rn, and its short half-life of 56 seconds effectively precludes diffusion of the gas away from the site of radioactive decay.) Potassium concentration should not change either, but the "potassium" count rates are strongly affected by Compton scattering of uranium gamma rays. After stripping to remove these gamma rays, the potassium concentrations inevitably have large uncertainties. Stripping of uranium from thorium is minimal; hence, the calculated thorium concentrations should be effectively constant. By mathematically adjusting the calculated thorium concentrations to a constant value, the variations in detector efficiency can be removed almost entirely. This was done for pad 4; the thorium concentrations in Table 4 were normalized to their average value, and the normalization factors were used to adjust the uranium concentrations. The results are shown in Figure 17, where the uranium concentrations given are those obtained after normalization to constant values of thorium concentration. The apparent uranium concentrations still show a significant increase during the winter months. (The low point for 11/18/77 in Figure 17 is directly due to the high thorium determined for that date; clearly, the high thorium value is erroneous. The high uranium concentration calculated for 1/25/78 probably is related to the snow cover on the ground adjoining the pads, which was unique to that date.) The continued existence of the uranium increase after normalization to constant thorium makes it highly improbable that the detection system is the origin of these changes. It thus appears that radon variations are the only explanation for the changes in apparent uranium concentrations of the pads.

TABLE 4.
PAD CONCENTRATIONS CALCULATED FROM MONITORING DATA
(%K, ppm U, ppm Th)

PAD	ELEMENT	10/17/77	10/31/77	11/18/77	12/01/77	12/14/77	01/09/78	01/25/78	02/03/78	03/08/78	04/07/78	04/12/78
1	K	1.61 ± 0.01	1.57 ± 0.01	*	1.60 ± 0.01	1.61 ± 0.01	1.57 ± 0.01	1.57 ± 0.01	1.60 ± 0.01	1.58 ± 0.01	1.58 ± 0.01	1.59 ± 0.01
	U	3.46 ± 0.05	3.38 ± 0.05	*	3.07 ± 0.05	3.36 ± 0.05	3.56 ± 0.05	3.77 ± 0.05	3.51 ± 0.05	2.96 ± 0.05	2.61 ± 0.04	2.59 ± 0.04
	Th	7.71 ± 0.09	7.75 ± 0.09	*	7.82 ± 0.09	7.48 ± 0.08	7.50 ± 0.08	7.47 ± 0.08	7.53 ± 0.08	7.47 ± 0.08	7.55 ± 0.08	7.46 ± 0.08
2	K	5.33 ± 0.02	5.23 ± 0.02	5.34 ± 0.02	5.25 ± 0.02	5.26 ± 0.02	5.21 ± 0.02	5.22 ± 0.02	5.24 ± 0.02	5.22 ± 0.02	5.29 ± 0.02	5.26 ± 0.02
	U	6.25 ± 0.08	6.55 ± 0.08	6.20 ± 0.08	6.15 ± 0.08	6.25 ± 0.08	6.70 ± 0.08	6.98 ± 0.08	6.36 ± 0.08	6.02 ± 0.08	5.33 ± 0.07	5.23 ± 0.07
	Th	9.91 ± 0.12	9.92 ± 0.12	10.80 ± 0.13	9.91 ± 0.12	9.86 ± 0.12	9.60 ± 0.12	9.45 ± 0.12	9.51 ± 0.12	9.60 ± 0.12	9.75 ± 0.12	9.76 ± 0.12
3	K	2.23 ± 0.02	2.12 ± 0.02	2.21 ± 0.02	2.18 ± 0.02	2.20 ± 0.02	2.13 ± 0.02	2.09 ± 0.02	2.13 ± 0.02	2.16 ± 0.02	2.18 ± 0.02	2.17 ± 0.02
	U	6.48 ± 0.12	6.20 ± 0.11	6.17 ± 0.12	6.22 ± 0.11	6.81 ± 0.12	6.62 ± 0.12	7.29 ± 0.12	6.50 ± 0.11	6.02 ± 0.11	5.79 ± 0.11	5.28 ± 0.11
	Th	47.49 ± 0.26	47.51 ± 0.26	47.84 ± 0.26	46.61 ± 0.26	46.47 ± 0.26	46.62 ± 0.26	46.38 ± 0.26	46.38 ± 0.26	46.12 ± 0.26	46.23 ± 0.26	46.29 ± 0.26
4	K	2.23 ± 0.02	2.03 ± 0.02	2.28 ± 0.02	2.17 ± 0.02	2.19 ± 0.02	2.12 ± 0.02	2.20 ± 0.02	2.10 ± 0.02	2.20 ± 0.02	2.21 ± 0.02	2.17 ± 0.02
	U	30.20 ± 0.15	30.55 ± 0.15	30.74 ± 0.15	31.74 ± 0.15	31.73 ± 0.15	32.51 ± 0.15	33.35 ± 0.15	32.15 ± 0.15	32.12 ± 0.15	29.89 ± 0.14	29.30 ± 0.14
	Th	10.72 ± 0.14	10.88 ± 0.14	11.49 ± 0.15	10.94 ± 0.14	10.75 ± 0.14	10.59 ± 0.14	10.34 ± 0.14	10.25 ± 0.14	10.37 ± 0.14	10.22 ± 0.14	10.41 ± 0.14
5	K	4.40 ± 0.02	4.27 ± 0.02	4.40 ± 0.02	4.28 ± 0.02	4.37 ± 0.02	4.30 ± 0.02	4.21 ± 0.02	4.30 ± 0.02	4.30 ± 0.02	4.29 ± 0.02	4.33 ± 0.02
	U	21.13 ± 0.13	22.22 ± 0.13	21.77 ± 0.13	22.40 ± 0.13	22.43 ± 0.13	22.84 ± 0.13	23.63 ± 0.14	22.99 ± 0.14	22.41 ± 0.13	20.50 ± 0.13	20.19 ± 0.13
	Th	19.90 ± 0.18	19.81 ± 0.18	19.73 ± 0.18	19.54 ± 0.18	19.73 ± 0.18	19.28 ± 0.18	19.22 ± 0.18	19.14 ± 0.18	19.14 ± 0.18	19.36 ± 0.18	19.56 ± 0.18

Note: Statistical uncertainties quoted are the 95% confidence intervals from the counting data. Uncertainties in the detector's response matrix are constant; these uncertainties are not included in this table.

* Data unavailable due to magnetic tape error.

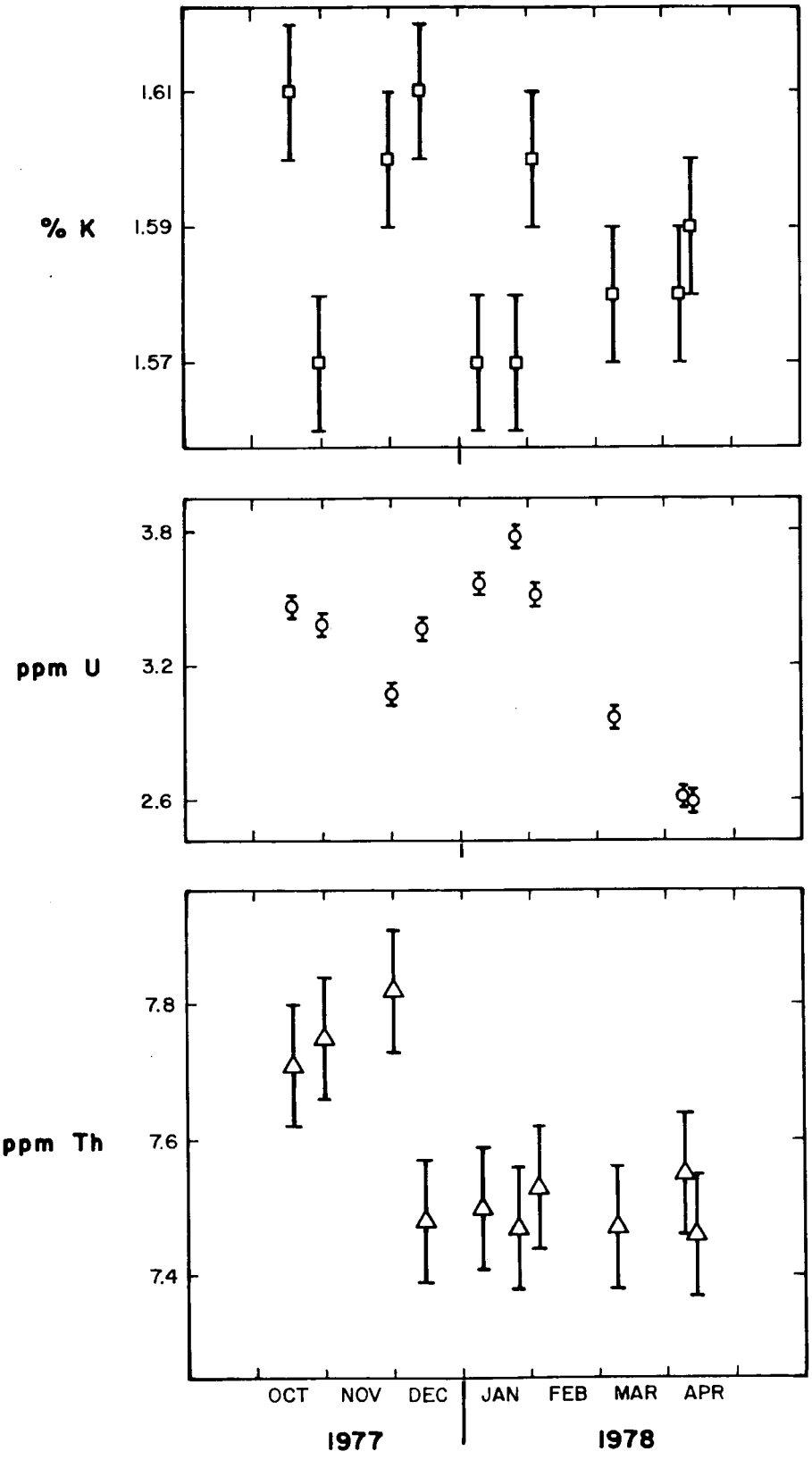

FIGURE 11.
PAD 1 CALCULATED CONCENTRATIONS FROM OCTOBER 1977 TO APRIL 1978

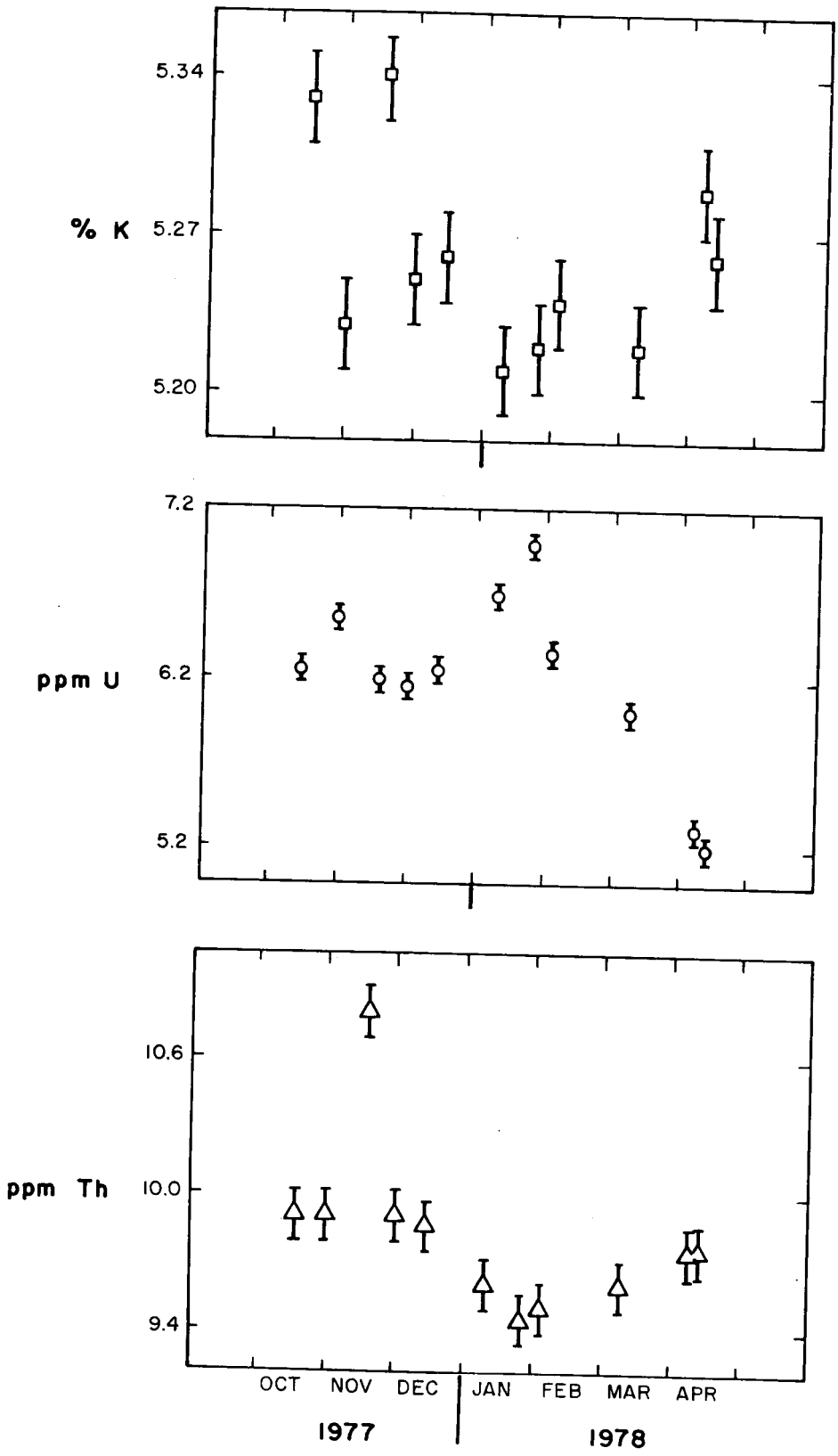

FIGURE 12.
PAD 2 CALCULATED CONCENTRATIONS FROM OCTOBER 1977 TO APRIL 1978

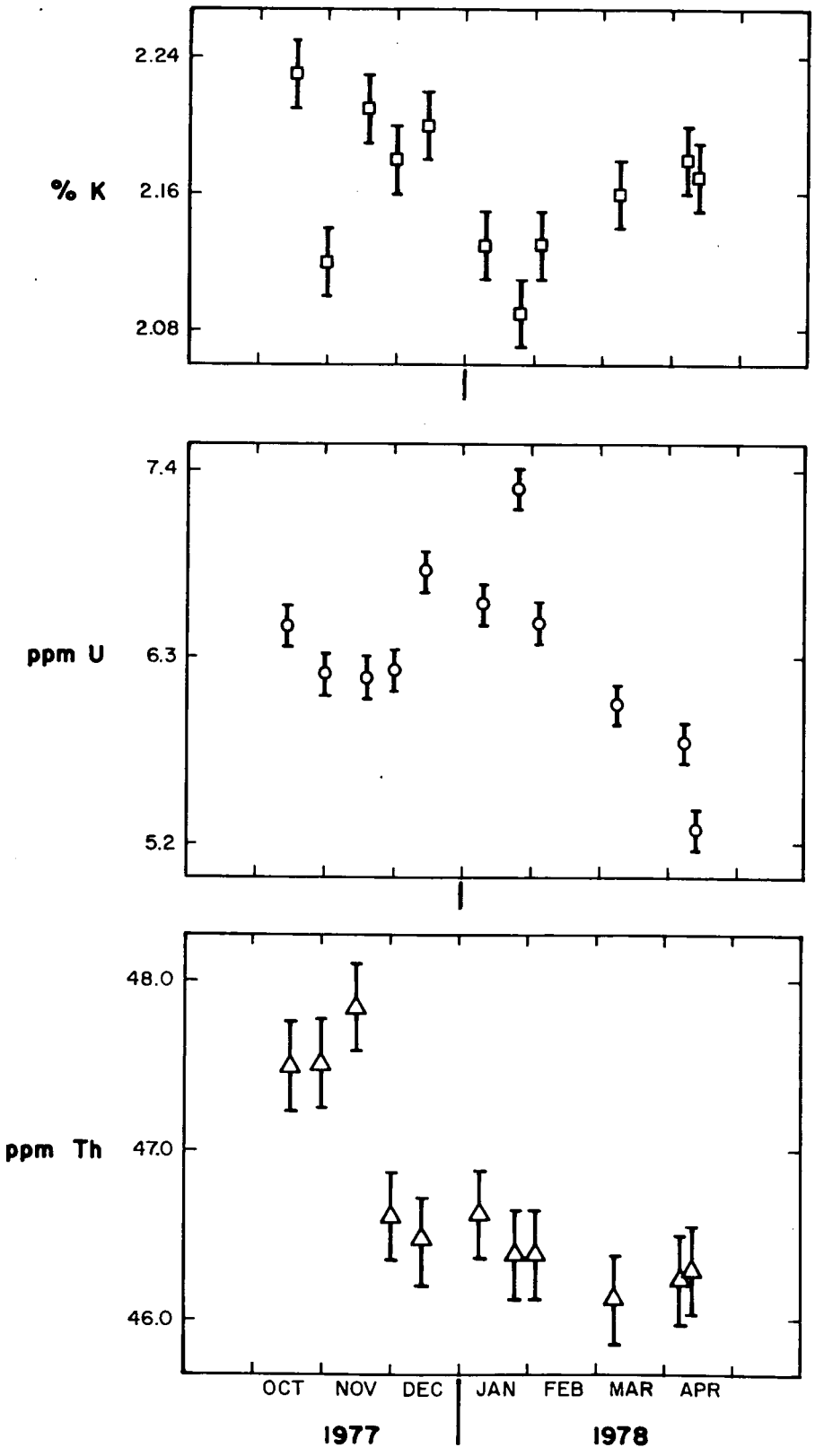

FIGURE 13.
PAD 3 CALCULATED CONCENTRATIONS FROM OCTOBER 1977 TO APRIL 1978

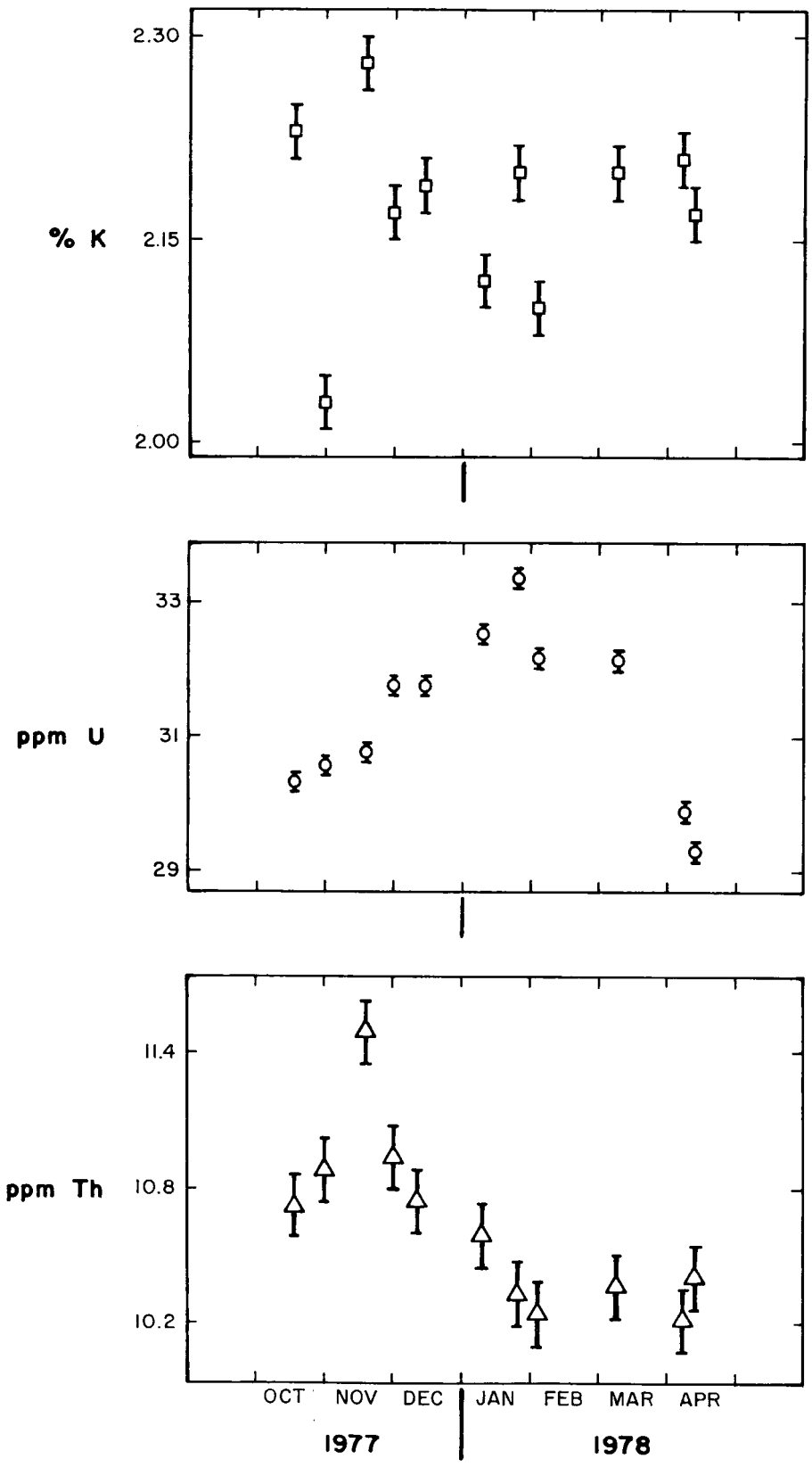

FIGURE 14.
PAD 4 CALCULATED CONCENTRATIONS FROM OCTOBER 1977 TO APRIL 1978

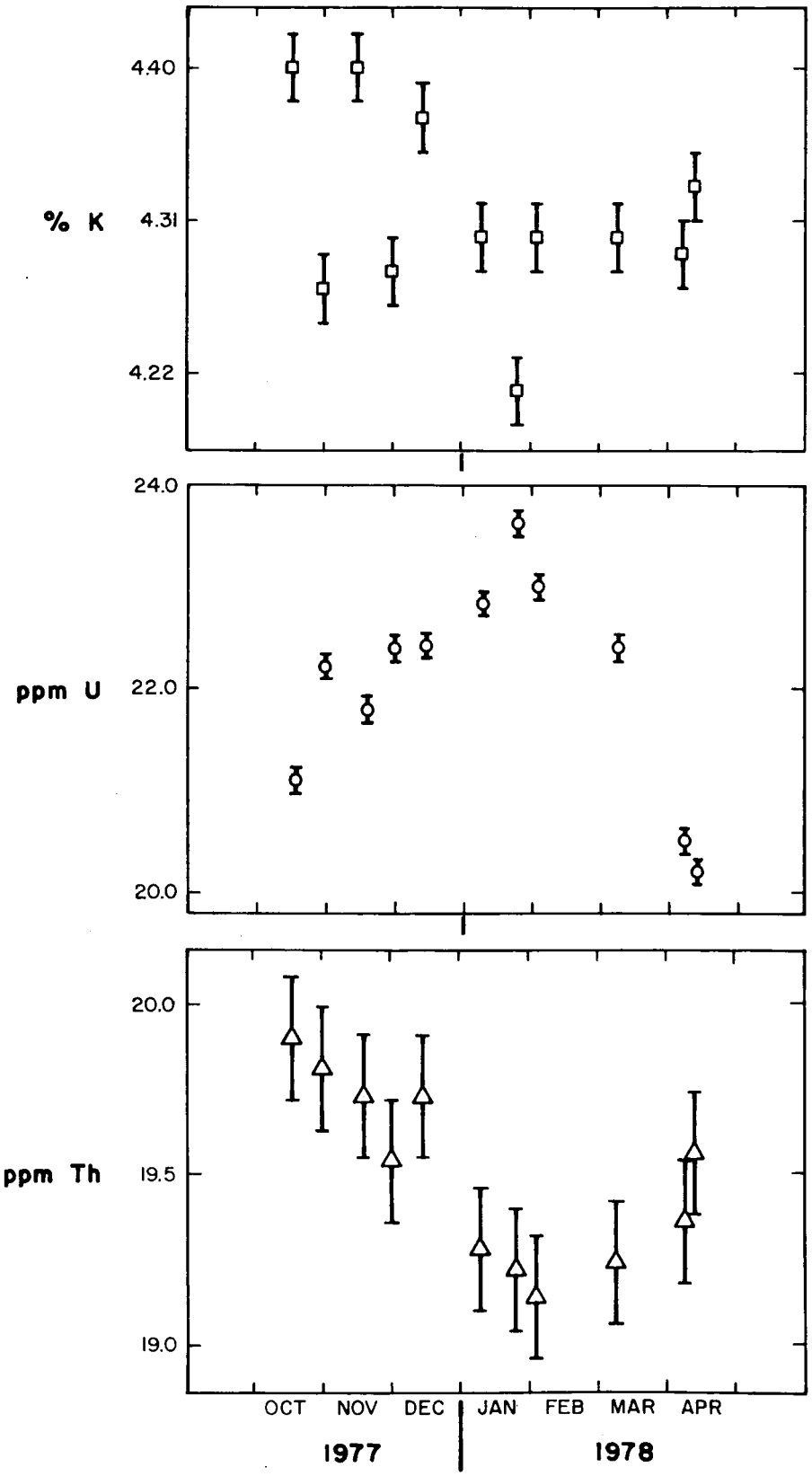

FIGURE 15.
PAD 5 CALCULATED CONCENTRATIONS FROM OCTOBER 1977 TO APRIL 1978

TABLE 5.
PAD CONCENTRATIONS CALCULATED FROM BACKGROUND-SUBTRACTED DATA—PAD 1 TAKEN AS BACKGROUND
(%K, ppm U, ppm Th)

PAD	ELEMENT	10/17/77	10/31/77	12/01/77	12/14/77	01/09/78	01/25/78	02/03/78	03/08/78	04/07/78	04/12/78
2	K	3.72 ± 0.02	3.66 ± 0.02	3.65 ± 0.02	3.66 ± 0.02	3.64 ± 0.02	3.65 ± 0.02	3.64 ± 0.02	3.65 ± 0.02	3.71 ± 0.02	3.67 ± 0.02
	U	2.79 ± 0.09	3.17 ± 0.09	3.08 ± 0.09	2.89 ± 0.09	3.15 ± 0.09	3.21 ± 0.09	2.85 ± 0.09	3.05 ± 0.09	2.72 ± 0.09	2.64 ± 0.09
	Th	2.20 ± 0.15	2.17 ± 0.15	2.09 ± 0.15	2.39 ± 0.15	2.11 ± 0.15	1.99 ± 0.15	1.97 ± 0.15	2.13 ± 0.15	2.20 ± 0.15	2.29 ± 0.15
3	K	0.61 ± 0.02	0.55 ± 0.02	0.58 ± 0.02	0.60 ± 0.02	0.56 ± 0.02	0.52 ± 0.02	0.53 ± 0.02	0.58 ± 0.02	0.59 ± 0.02	0.58 ± 0.02
	U	3.02 ± 0.13	2.83 ± 0.13	3.15 ± 0.13	3.45 ± 0.13	3.07 ± 1.13	3.52 ± 0.13	3.00 ± 0.13	3.06 ± 0.13	3.18 ± 0.13	2.69 ± 0.13
	Th	39.78 ± 0.28	39.77 ± 0.28	38.78 ± 0.28	38.99 ± 0.28	39.12 ± 0.28	38.91 ± 0.28	38.85 ± 0.28	38.64 ± 0.28	38.68 ± 0.28	38.83 ± 0.28
4	K	0.62 ± 0.03	0.46 ± 0.03	0.57 ± 0.03	0.59 ± 0.03	0.56 ± 0.03	0.63 ± 0.03	0.51 ± 0.03	0.62 ± 0.03	0.63 ± 0.03	0.58 ± 0.03
	U	26.73 ± 0.16	27.17 ± 0.16	28.67 ± 0.16	28.37 ± 0.16	28.96 ± 0.16	29.58 ± 0.16	28.64 ± 0.16	29.15 ± 0.16	27.27 ± 0.16	26.71 ± 0.16
	Th	3.01 ± 0.16	3.14 ± 0.16	3.11 ± 0.16	3.27 ± 0.16	3.09 ± 0.16	2.88 ± 0.16	2.72 ± 0.16	2.90 ± 0.16	2.66 ± 0.16	2.95 ± 0.16
5	K	2.79 ± 0.03	2.70 ± 0.03	2.69 ± 0.03	2.77 ± 0.03	2.73 ± 0.03	2.64 ± 0.03	2.71 ± 0.03	2.73 ± 0.03	2.71 ± 0.03	2.73 ± 0.03
	U	17.67 ± 0.15	18.34 ± 0.15	19.33 ± 0.15	19.08 ± 0.15	19.29 ± 0.15	19.87 ± 0.15	19.48 ± 0.15	19.45 ± 0.15	17.88 ± 0.15	17.60 ± 0.15
	Th	12.19 ± 0.20	12.07 ± 0.20	11.72 ± 0.20	12.26 ± 0.20	11.78 ± 0.20	11.76 ± 0.20	11.61 ± 0.20	11.76 ± 0.20	11.81 ± 0.20	12.10 ± 0.20

Note: Statistical uncertainties are the 95% confidence intervals from the counting data. Uncertainties in the detector's response matrix are constant; these uncertainties are not included in this table.

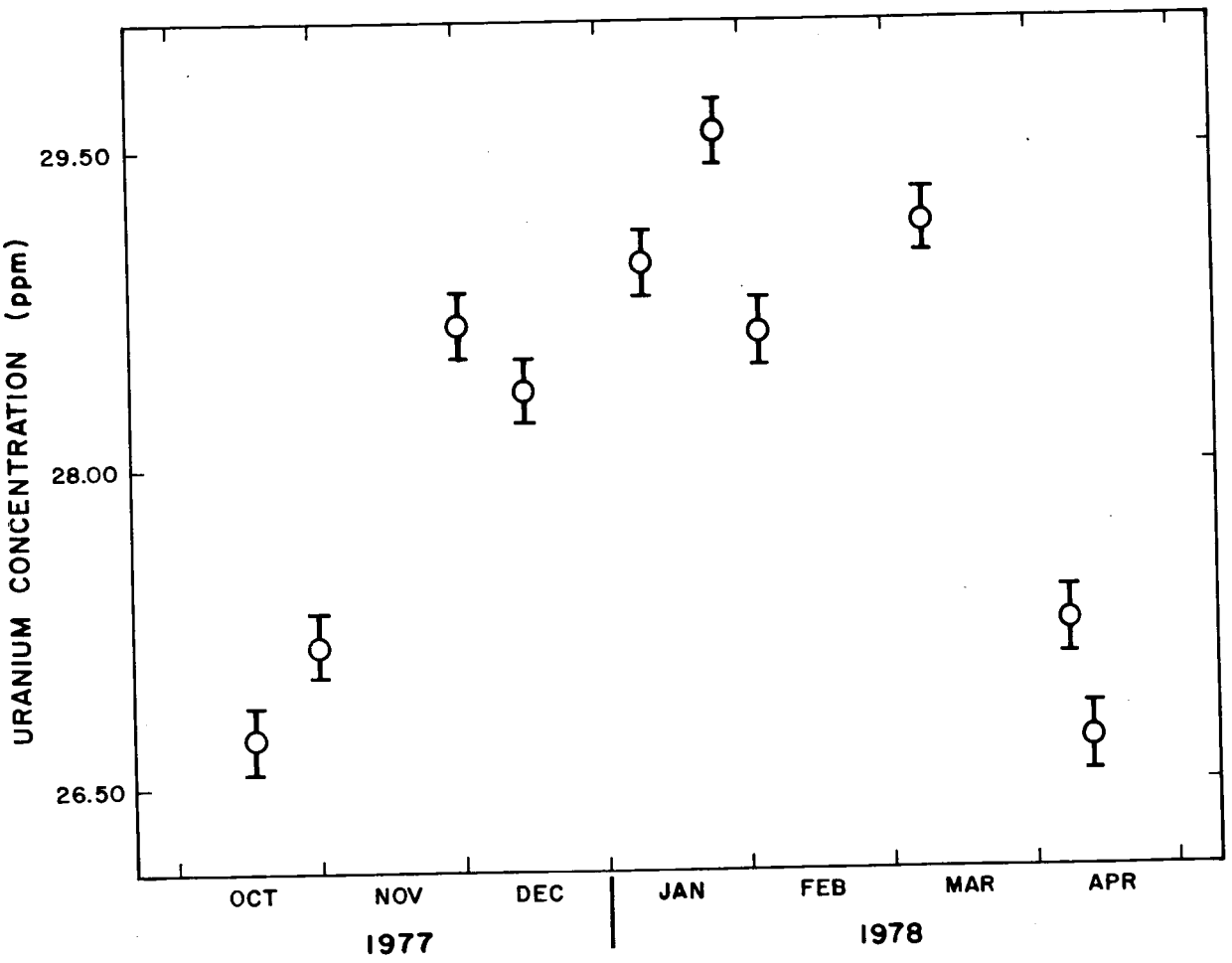

FIGURE 16.
APPARENT URANIUM CONCENTRATION OF PAD 4 AFTER BACKGROUND SUBTRACTION

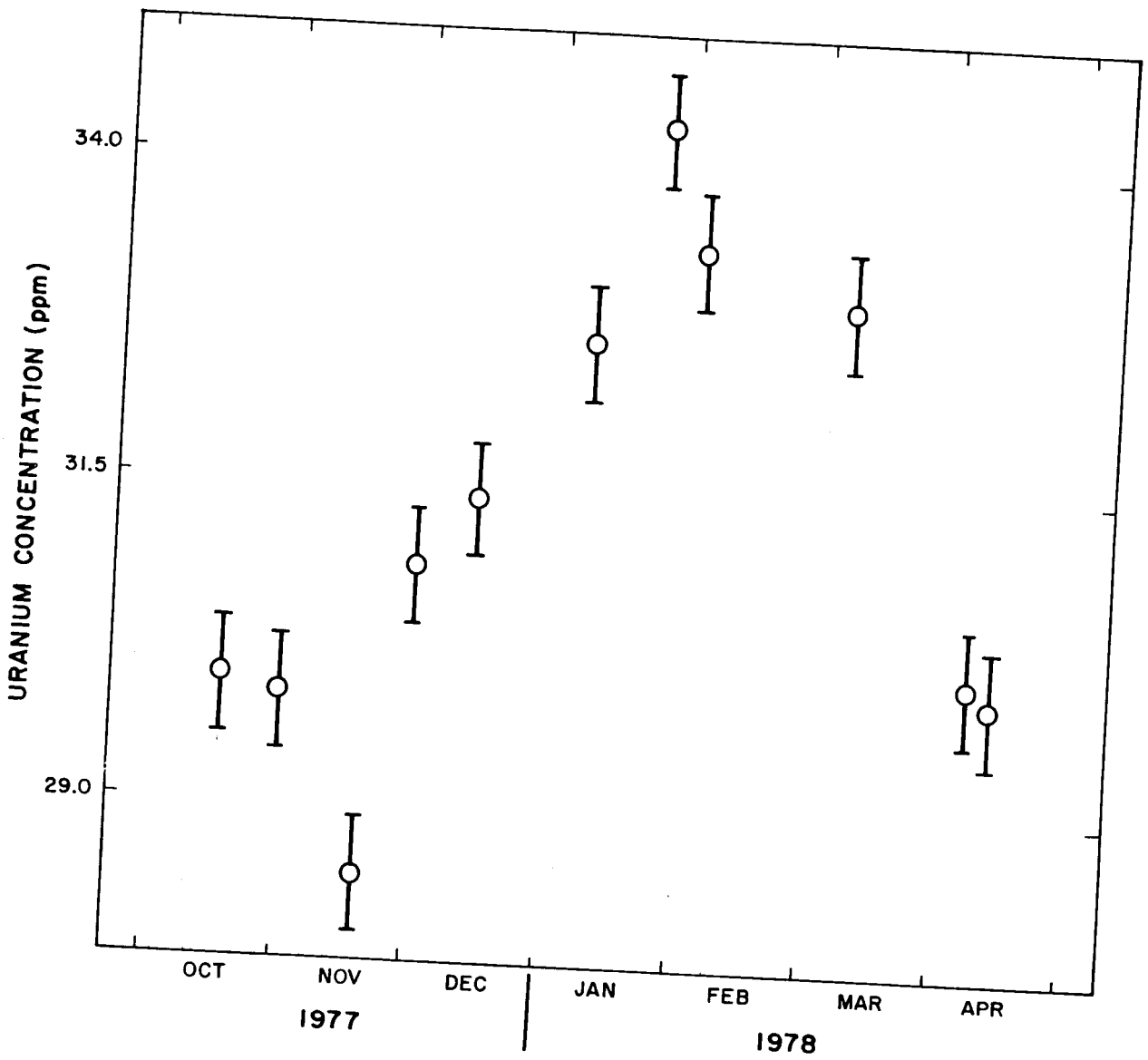

FIGURE 17.
APPARENT URANIUM CONCENTRATION OF PAD 4
AFTER NORMALIZATION TO CONSTANT THORIUM CONCENTRATION

METEOROLOGICAL EFFECTS

The variation in apparent uranium concentration is most certainly due to radon concentration changes within the pads. Because the changes appear to be seasonal, it is reasonable to investigate meteorological effects on the radon in the pads. The location of the pads at the Grand Junction airport, where a weather service office of the National Oceanic and Atmospheric Administration (NOAA) is present, provides access to weather data. NOAA meteorological data for the radiation monitoring period have been obtained in an attempt to find a correlation between the weather and the radon variations. The following variables have been investigated: temperature, barometric pressure, precipitation, and relative humidity.

Temperature

The temperatures during the radiation monitoring are shown in Figure 18. Comparison of these temperatures with the apparent uranium concentrations in Figure 17 shows a trend to lower temperatures in the winter when the uranium concentrations are enhanced, but there is no point-by-point correlation evident between temperature and uranium concentration. For example, the uranium data for the dates 10/17/77 and 10/31/77 are almost the same, but the temperatures are much different. Air temperature alone does not appear to be able to account for the daily radon variations. However, it is well known that increased concentrations of airborne radon can accumulate near the earth's surface during temperature inversions (Evans, 1959).

Barometric Pressure

Barometric pressure can be expected to affect the radon in the pads by pumping the radon out when the barometric pressure decreases. Studies have been performed on barometric pumping of radon through soil from an underlying orebody (Jeter et al, 1977; Clements and Wilkening, 1974; Tanner, 1978), but the applicability of these results to the concrete airport pads is not readily evident. Figure 19 shows the barometric pressure at the time of the radiation monitoring, and Figure 20 gives the change in barometric pressure for the 24 hours preceeding the radiation monitoring. No clear correlation with the apparent uranium concentration is evident for either the pressure at the time of monitoring or for the change in barometric pressure during the preceeding 24 hours. As an example, the apparent uranium concentrations are almost the same on 10/17/77 and 4/7/78, but the barometric pressures are quite different for these dates. In addition, the barometric pressure changes for November 1977 through March 1978 generally have the wrong sign to support a model of barometric pumping of radon; their negative signs suggest removal of radon from the pads and a decrease in apparent uranium concentration rather than the observed increase in apparent uranium concentration for those months.

Precipitation

Precipitation at the pads prior to monitoring could influence the escape of radon from the pads by creating a moisture barrier. The amount of precipitation during the 4 days prior to the monitorings is plotted in Figure 21. Again there appears to be no strong correlation with the radiometric data. For example, the large amount of rain received before the monitoring on 4/12/78 did not increase the apparent uranium reading as would have been expected. Apparently the rain during the days preceeding monitoring did not have any direct influence on the radon emanation from the pads. The precipitation shown in Figure 21 occurred two or three days prior to the monitoring because the days selected for monitoring were those on which the pads were dry, and no significant precipitation had occurred for at least a day preceeding the monitoring. Possibly, precipitation closer to the actual monitoring time would affect the radon emanation. The extreme case of having water standing on the pads was discussed earlier; in that case, the standing water apparently trapped the radon below its surface.

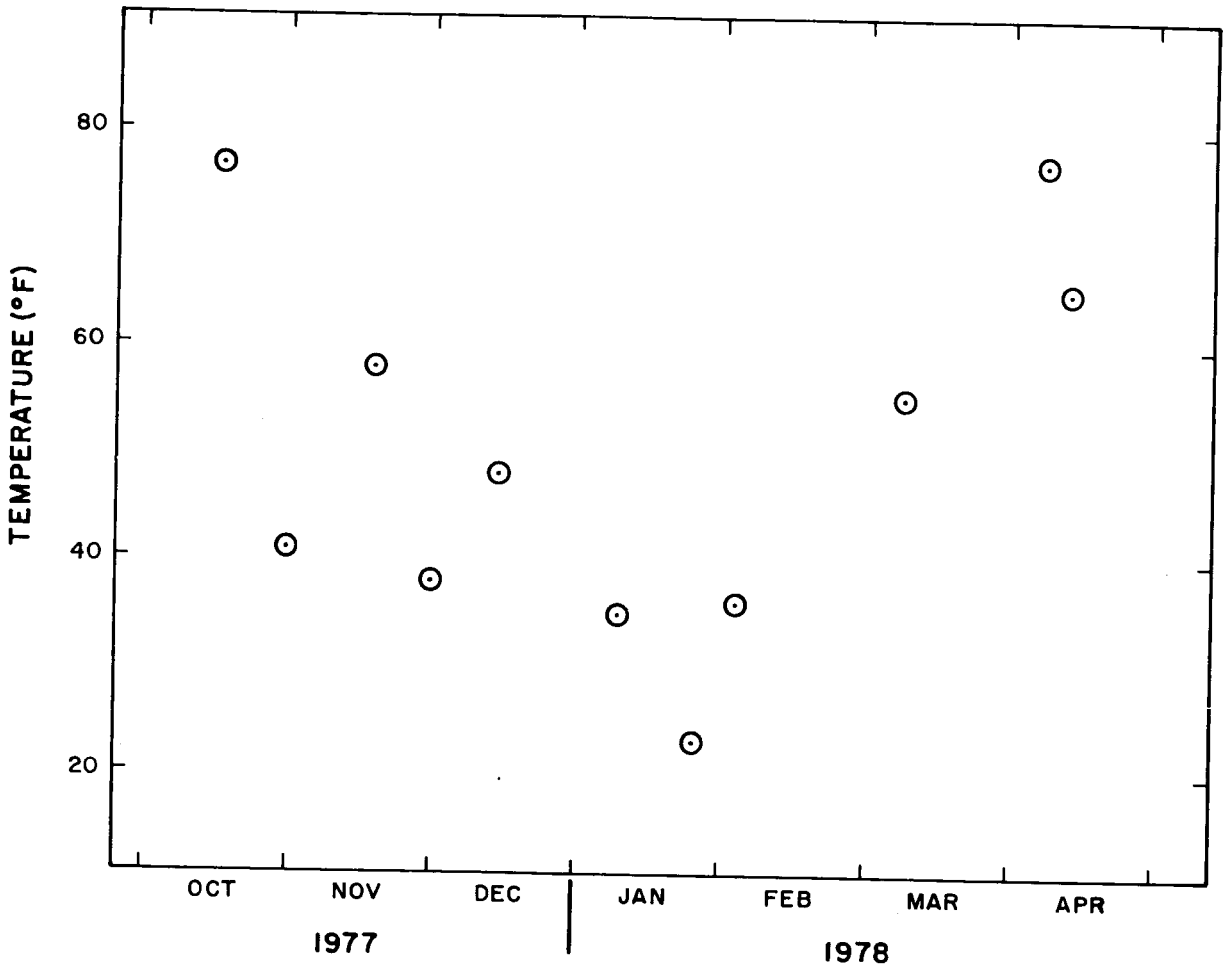

FIGURE 18.
TEMPERATURES FOR RADIATION MONITORING DATES
(Readings taken at 1400 hours)

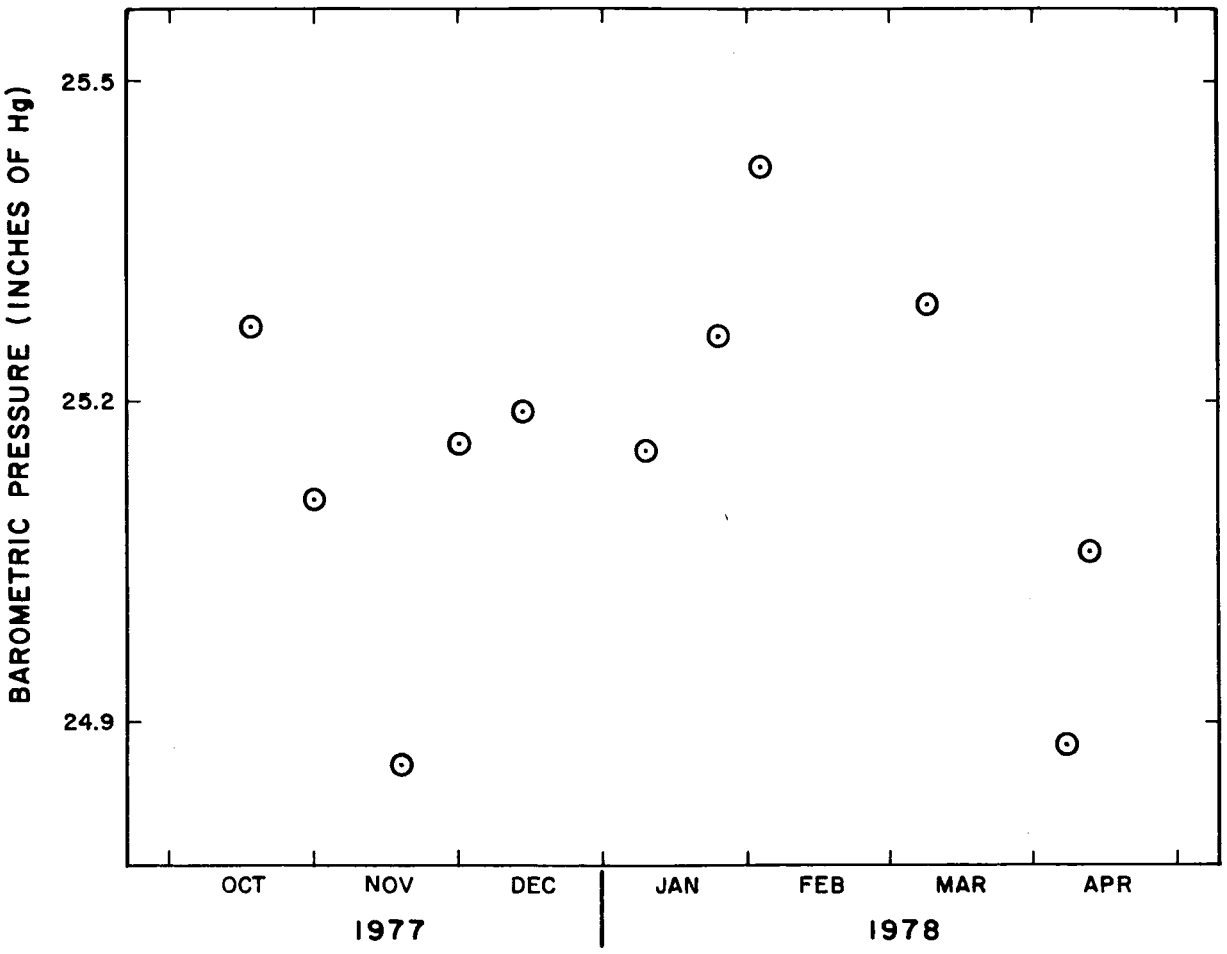

FIGURE 19.
BAROMETRIC PRESSURE DURING RADIATION MONITORING

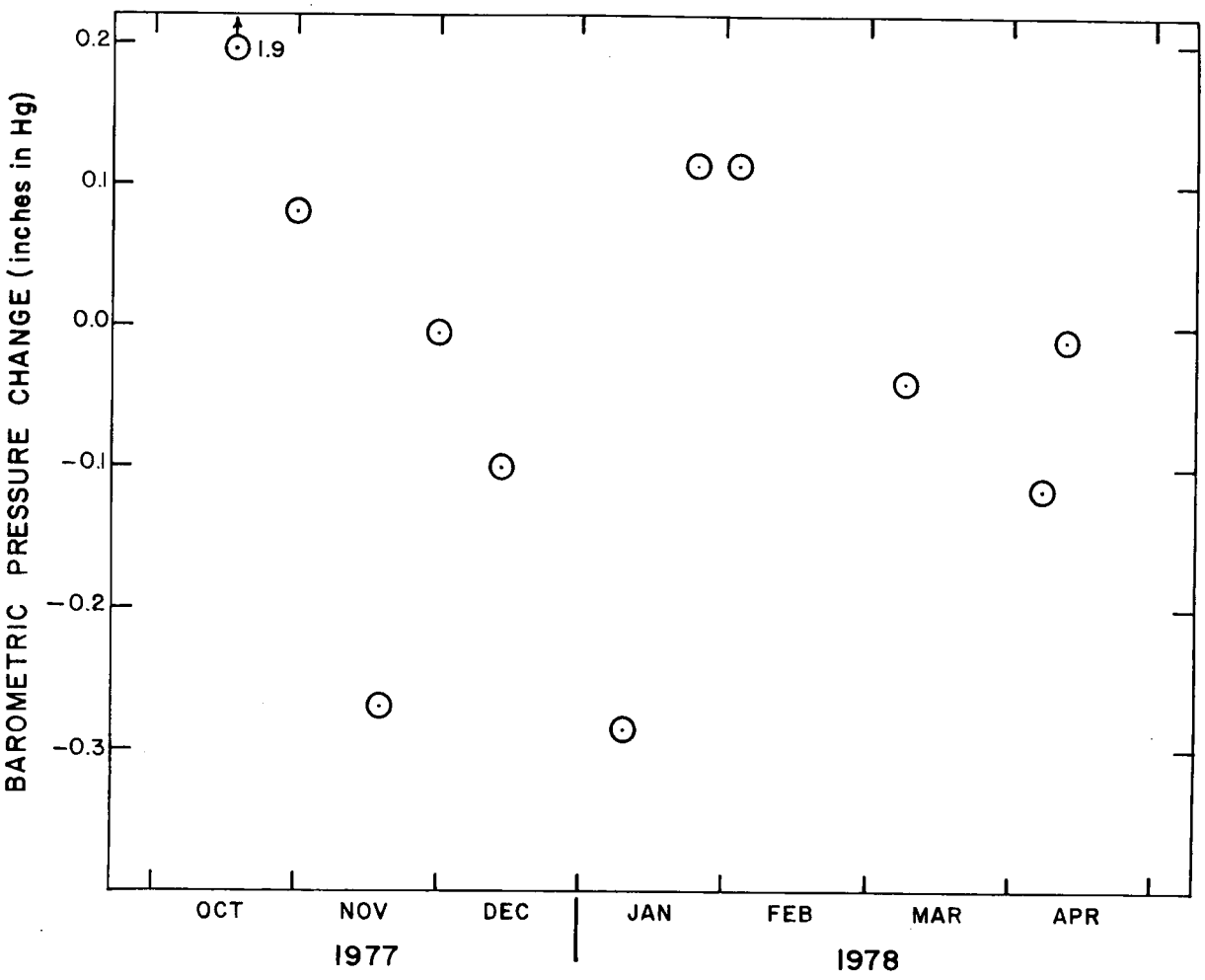

FIGURE 20.
CHANGE IN BAROMETRIC PRESSURE FOR THE 24 HOURS PRECEEDING RADIATION MONITORING

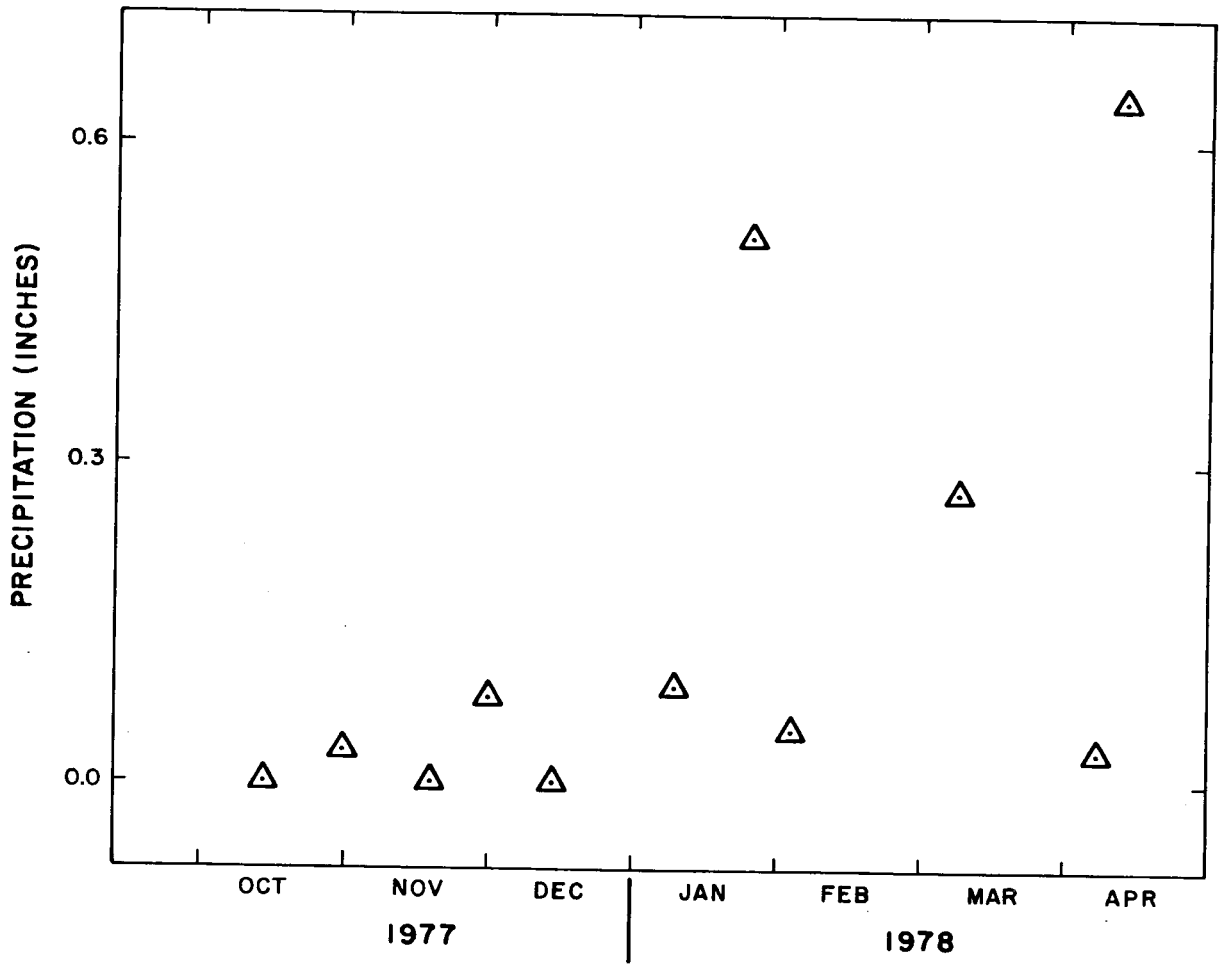

FIGURE 21.
PRECIPITATION PRIOR TO RADIATION MONITORING

Relative Humidity

Relative humidity is the percent of water vapor in the air relative to the amount of water vapor that the air can hold at a given temperature. The relative humidity at the time of the pad monitorings is given in Figure 22. (The high relative humidity on 10/31/77 was a jump in humidity due to a slight trace of rain during the monitoring.) The relative humidity on the monitoring days follows the same trend as does the uranium radiation shown in Figures 16 and 17. On days when the relative humidity is high, the calculated apparent uranium concentration also is generally high. The relative humidity prior to the monitoring time might be expected to be related to the radon emanation also. Figure 23 shows the humidity early in the mornings on the monitoring days as well as on the previous day. These humidities show the same trend as does the uranium radiation. In general the data show that the humidity does not change rapidly and that there appears to be a relationship between relative humidity and the apparent uranium concentration of the pads.

The relative humidity of the air above the pads seems to affect the radon migration from the pads. Perhaps the pore spaces in the concrete at the surface of the pads contain air which tends to reach an equilibrium in humidity with that of the adjoining atmosphere. The addition of moisture to these pore spaces can act as a barrier to radon migration from the pads. Rain should produce the same effect of increasing the moisture in the upper pore spaces of the pads. The time delay between precipitation and radiation measurements, however, apparently was sufficient to destroy this correlation. The lack of correlation with precipitation also suggests little soaking of the rain deep into the pads. It seems clear that the changing moisture in the surface of the concrete does affect the radon escape from the pads; however, the means by which the moisture is transferred in and out of the pads is not well known. The relative humidity of the surrounding air seems to be related to this transfer more strongly than does actual precipitation, at least when the pads are measured with a dry surface.

More work is required on relating meteorological variables to radon emanation. The data collected at the airport pads are not adequate for this detailed meteorological investigation because there is no control over the meteorological variables. Laboratory experiments with concrete pad samples in environmental control chambers provide a means for independently adjusting the variables and observing the results. From these experiments it may be possible to determine a functional relationship between changes in radon emanation from the pads and the meteorological variables.

CONCLUSIONS

A program of periodic monitoring of the Walker Field airport pads has been established to determine their radiometric stability. For this purpose, a NaI detector and multichannel analyzer are used to obtain spectral data from the pads. The apparent uranium concentrations of the pads were found to increase by approximately 10 percent during the winter of 1978. These changes have been attributed to radon buildup in the pads. Meteorological causes for the radon variations were considered, and the relative humidity was found to provide a close correlation with the change in apparent uranium concentration.

At the present time, the radioelement concentrations assigned to the airport pads have fixed values, and they do not reflect the seasonal variations in the radon emanated from the pads. Eventually, it may be desirable to adjust the uranium concentrations to account for the observed variations in apparent uranium counts. However, more data should first be collected to quantify the changes and verify their consistency. Monitoring data for at least 18 months will be required for this purpose.

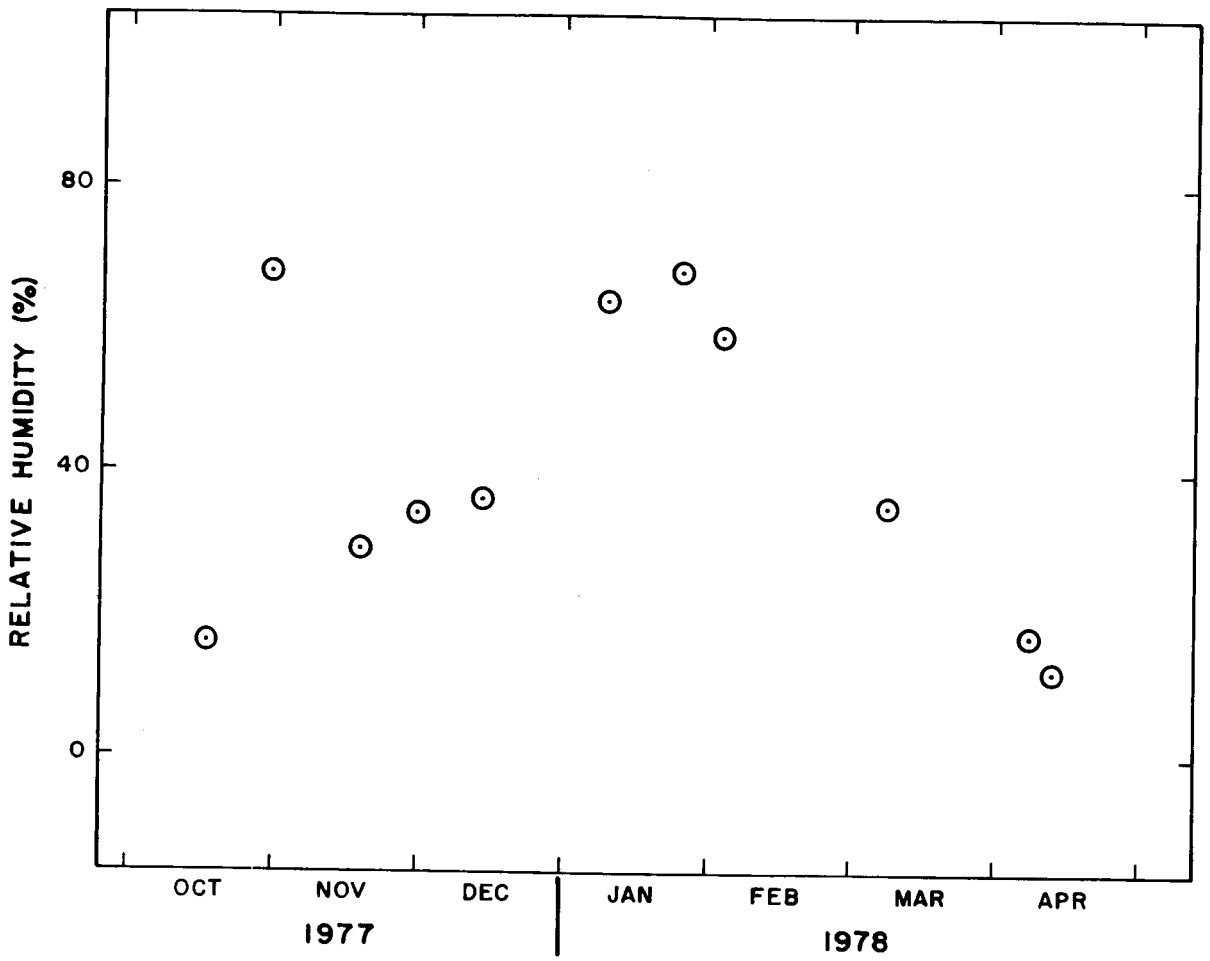

FIGURE 22.
RELATIVE HUMIDITY DURING RADIATION MONITORING

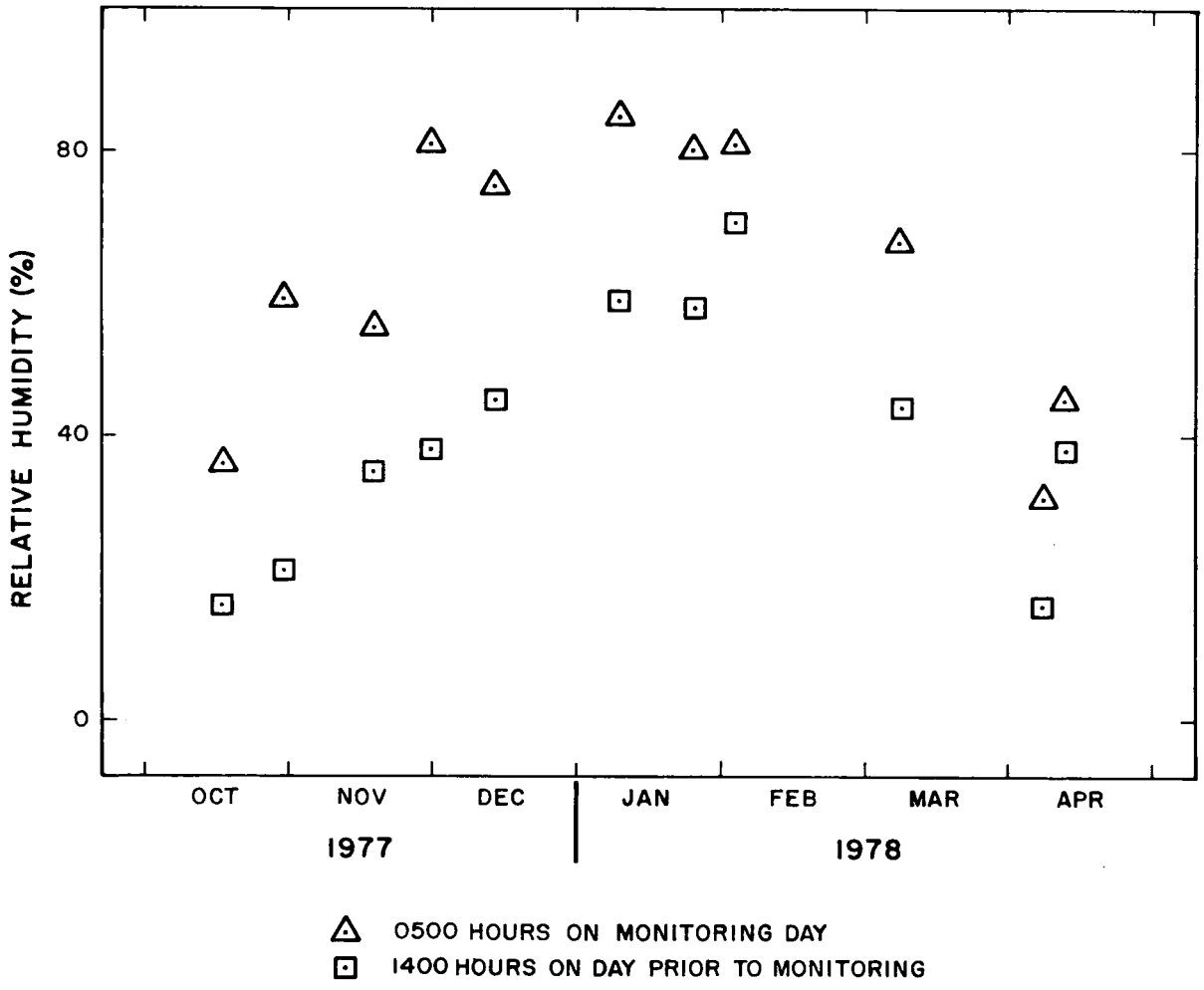

FIGURE 23.
RELATIVE HUMIDITY PRIOR TO RADIATION MONITORING

SELECTED REFERENCES

Clemens, W. E. and Wilkening, M. H., 1974, Atmospheric pressure effects on ^{222}Rn transport across the earth-air interface: Journal of Geophysical Research, v. 79, p. 5025.

Evans, H. B., 1959, Measurements of natural atmospheric radioactivity over geologic features with carborne apparatus: U.S. Geological Survey Internal Report.

Jeter, H. W., Martin, J. D., and Schutz, D. F., 1977, The migration of gaseous radionuclides through soil overlying a uranium ore deposit: a modeling study: Bendix Field Engineering Corporation Open-File Report No. GJBX-67(77), U.S. Department of Energy, Grand Junction, Colorado.

Løvborg, L., Bøtter-Jensen, L., and Kirkegaard, P., 1978, Experences with concrete calibration sources for radiometric field instruments: Geophysics, v. 43, p. 543-49.

Stromswold, D. C. and Kosanke, K. L., 1978, Calibration and error analysis for spectral radiation detectors: IEEE Transactions on Nuclear Science, v. NS-25, #1, p. 782-86.

Tanner, A. B., 1978, Radon migration in the ground: a supplementary review: paper presented at The Natural Radiation Environment III, 23-28 April 1978, University of Texas, Houston.

Ward, D. L., 1978, Construction of the calibration pads facility, Walker Field, Grand Junction, Colorado: Bendix Field Engineering Corporation Open-File Report No. GJBX-37(78), U.S. Department of Energy, Grand Junction, Colorado.